A SEMI-PORTABLE SHEET METAL FLUME

FOR AUTOMATED IRRIGATION

By

VINCENT W. UHL JR.

Bachelor of Science

University of Notre Dame

Notre Dame, Indiana

1966

Submitted to the Faculty of the Graduate College
of the Oklahoma State University
in partial fulfillment of the requirements
for the Degree of
MASTER OF SCIENCE
May, 1970

A SEMI-PORTABLE SHEET METAL FLUME

FOR AUTOMATED IRRIGATION

Thesis Approved:

James E. Gartons
Thesis Adviser

F. R. Crow

D. Durham
Dean of the Graduate College

ACKNOWLEDGMENTS

The research reported in this thesis was financed in part by the United States Department of the Interior as authorized under Public Law 88-379. This research was conducted as a project of the Oklahoma Water Resources Research Institute (Okla. - A-015), Dr. Marvin T. Edminson, Director. The financial support of the Institute is appreciated.

The author is grateful to the Department of Agricultural Engineering, headed by Professor E. W. Schroeder, for furnishing the assistantships which made the work and study possible.

A deep feeling of appreciation is extended to the author's adviser, Dr. James E. Garton, for his competent guidance, stimulation, and help during the course of the entire project.

The author is also thankful to Mr. W. O. Ree, Engineer in Charge of the Outdoor Hydraulic Laboratory, Agricultural Research Service of the United States Department of Agriculture, for granting access to the experimental facilities. Other members of the Outdoor Hydraulic Laboratory staff are thanked for their cooperation and helpful suggestions during the course of the project. Draftsmen, Mr. Jack Fryrear and Mr. Norman Griffin, are thanked for their excellent work in preparing illustrative materials. Mr. Clyde Skoch, Mr. Norvil Cole, and Mr. Jess Hoisington of the Agricultural Engineering Research Laboratory are thanked for their helpful suggestions and cooperation.

The useful comments and suggestions from fellow graduate students

were appreciated.

The help of undergraduate David Pope with the construction and testing of the project was excellent; also the help of undergraduate Terry Allen during the testing was excellent. Both men did an outstanding job during the duration of the project, and the author is indebted to them.

Sincere thanks to Mrs. Linda Carlson for typing the rough draft, and to Mrs. Karen Metz for her conscientious typing of the final thesis.

The author would also like to recognize and thank Mr. Babubhai Khotari of Palanpur, India. Many hours were spent working and learning with Babubhai, and the author's initial interest in water development was stimulated by Babubhai.

Finally, the author would like to thank Estella Balmaceda for her help and inspiration.

TABLE OF CONTENTS

LIST OF TABLES

LIST OF FIGURES

CHAPTER I

INTRODUCTION

The Problem

Traditional surface irrigation is inhibited by high labor costs and low water application efficiency (normally in the fifty per cent range).

Surface irrigation systems usually utilize earthen or concrete channels or gated pipe. Earthen channels have the problem of high roughness coefficients, seepage, and require constant repair and maintenance. Concrete channels, while retarding seepage and having few maintenance problems, have the disadvantage of being permanent and hence not always adaptable to variable and changing cropping systems. Also, concrete channels put a certain amount of acreage out of production and hinder machine mobility. Gated pipe systems, while being mobile, have the problems of unequal furrow discharge, cost, and limited capacity.

Another problem basic to a furrow irrigation system is that furrow flows are uneven. That is, furrows being irrigated simultaneously receive water at different rates causing both insufficient applications and tailwater waste since flow is a function of head. Uniform discharge from a set of siphon tubes or weirs can be achieved if the siphon tubes or weirs discharging the flow have the same head.

Garton (7) designed an automated cut-back irrigation system which dealt with the problem of non-uniform furrow flow in the distribution bay. Rather than have a sloping channel, he designed a system that consisted of a series of horizontal bays staircased down the slope of a field. In a horizontal bay, a near horizontal water surface occurred and for siphon tubes at the same elevation, very uniform furrow flows resulted.

One problem with such a system is that the design of the system is dependent on a constant inflow Q, which can be difficult to maintain, especially where deep wells are used to supply the water. The system is also permanent and hence interferes with machine mobility, especially during planting and harvesting operations. The system is also difficult to adapt to changed cropping patterns.

A semi-portable irrigation channel designed with the functions of a cut-back system would have certain advantages. The channel could be set up after the planting season prior to the first irrigation and removed before harvesting. Such a system would also be adaptable to a change in Q and could be relocated to cope with changes in cropping patterns.

Objectives

1. To hydraulically design a portable irrigation channel to function as a cut-back system and to function automatically.

2. To structurally design and construct the channel.

3. To determine an average roughness coefficient for gradually varied flow.

4. To determine an average roughness coefficient for decreasing

spatially varied flow.

5. To determine the discharge characteristics of the orifice in the channel.

6. To determine discharge uniformity.

CHAPTER II

REVIEW OF LITERATURE

Automatic Surface Irrigation

In a response to the need for more efficient and labor saving irrigation systems, several researchers have done work on various aspects of automated irrigation.

Bondurant and Humphreys (4) described methods of automating irrigation systems. According to them, a completely automatic system would be a system which would:

1. Sense the need for irrigation;
2. Turn on the water if supplied from farm sources or request water if operating under a canal system;
3. Receive the water from the canal or other source and correctly irrigate the field portion by portion, or border by border; and
4. Turn off the water and reset itself so that the system would be prepared for the next irrigation.

The basic components of such a system includes:

1. Properly prepared fields;
2. Sensors or timers to regulate the cut-off system;
3. Accurately designed distribution systems.

Garton (7) developed an automated cut-back furrow irrigation system. A cut-back system uses a large furrow flow to initially wet the length of the furrow. After the initial wetting and before

tailwater flow occurs, the flow is reduced to balance the intake rate of the soil for that length of furrow.

Figure 1 shows a drawing of the system. A trapezoidal concrete ditch is used as the furrow distribution channel. The ditch consists of horizontal bays which follow the slope of the land in steps. Before the start of an irrigation, automated check gates are installed at the downstream end of each bay.

A typical irrigation sequence would be as follows: Water is turned into the ditch and rises in the first bay until it is discharging the initial furrow flow from each tube. When the furrows irrigated by this bay have irrigated through the field, the check dam automatically releases.

Water now enters the second bay and rises until the initial furrow flow is being discharged in the second bay, and the cut-back furrow flow is being discharged in the first bay. After the furrows in bay 2 are watered, the check dam releases automatically, and initial flow begins in bay 3 with cut-back flow in bay 2, and no furrow flow in bay 1.

Open Channel Flow, An Introduction

Most surface irrigation systems are a form of open channel flow. Open channel flow is characterized by a free surface, subject to atmospheric pressure.

The total energy in open channel flow, with reference to a datum line, is the sum of: the elevation, Z; i.e., the distance from the datum to the bottom of the channel; Y, the piezometric height; and $\frac{V^2}{2g}$, the velocity head; loss of energy is represented by h_f.

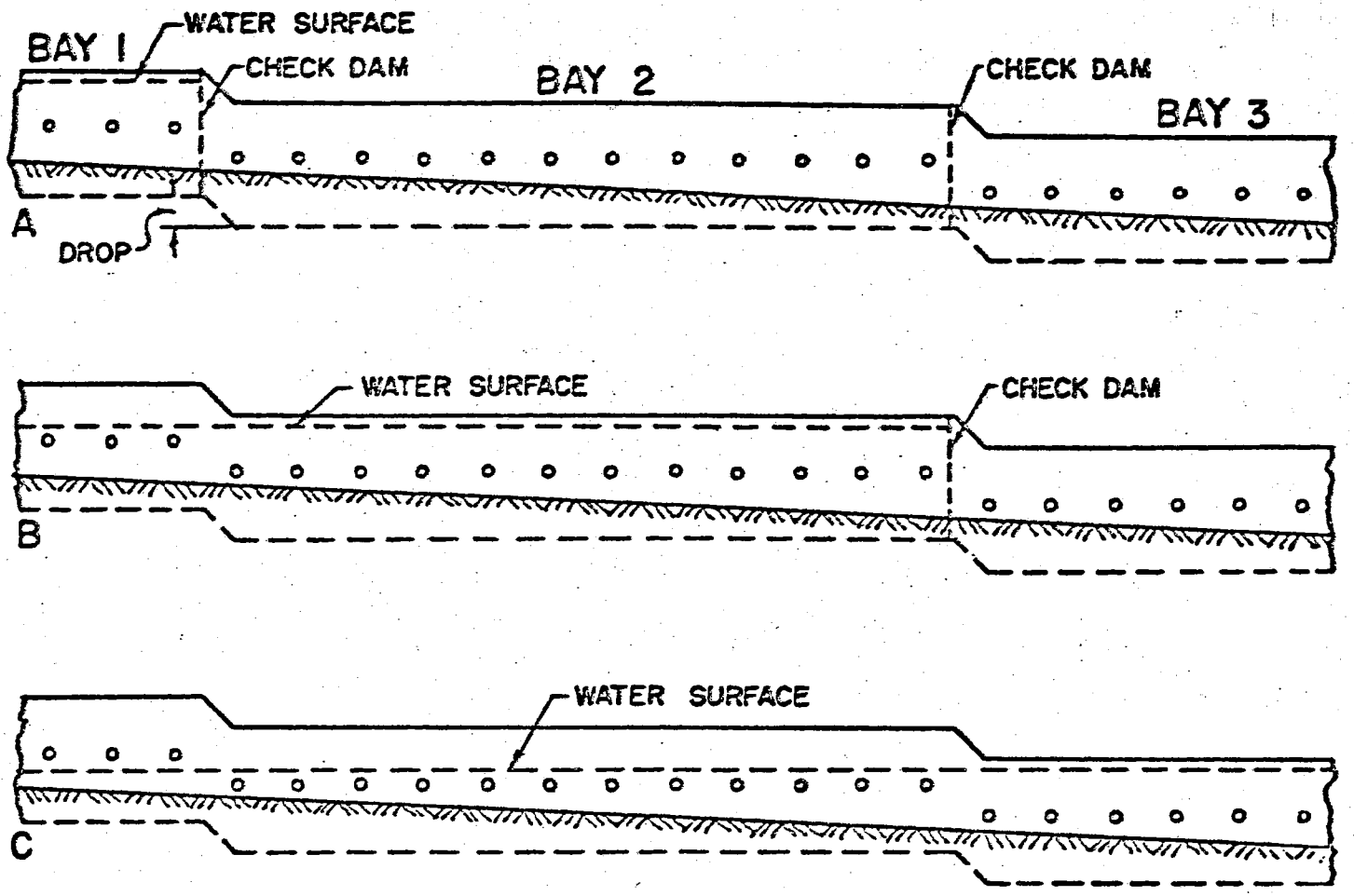

Figure 1. Elevation Drawing of Cut-Back Furrow Irrigation System Using one Cut-Back

Figure 2 gives a graphic description of total energy.

In general, the treatment of open channel flow is somewhat more empirical than closed conduit flow. This is because roughness varies from surface to surface and also the roughness in an open channel may vary with the position of the water surface.

Open channel flow is usually classified according to the change in flow depth with respect to time and place.

Steady and unsteady flow; time as the criterion.

$$\frac{dV}{dt} = 0, \quad X = \text{constant}$$

Steady flow occurs when the change in velocity with respect to time is zero, at X = constant. The flow is unsteady if the depth changes with time; i.e.,

$$\frac{dV}{dt} \neq 0, \quad X = \text{constant}$$

Uniform and non-uniform (varied) flow, space as the criterion.

$$\frac{dV}{dX} = 0, \quad t = \text{constant}$$

Uniform flow occurs when the change in velocity with respect to distance X is zero. The flow is non-uniform or varied if the depth changes with distance; i.e.,

$$\frac{dV}{dX} \neq 0, \quad t = \text{constant}$$

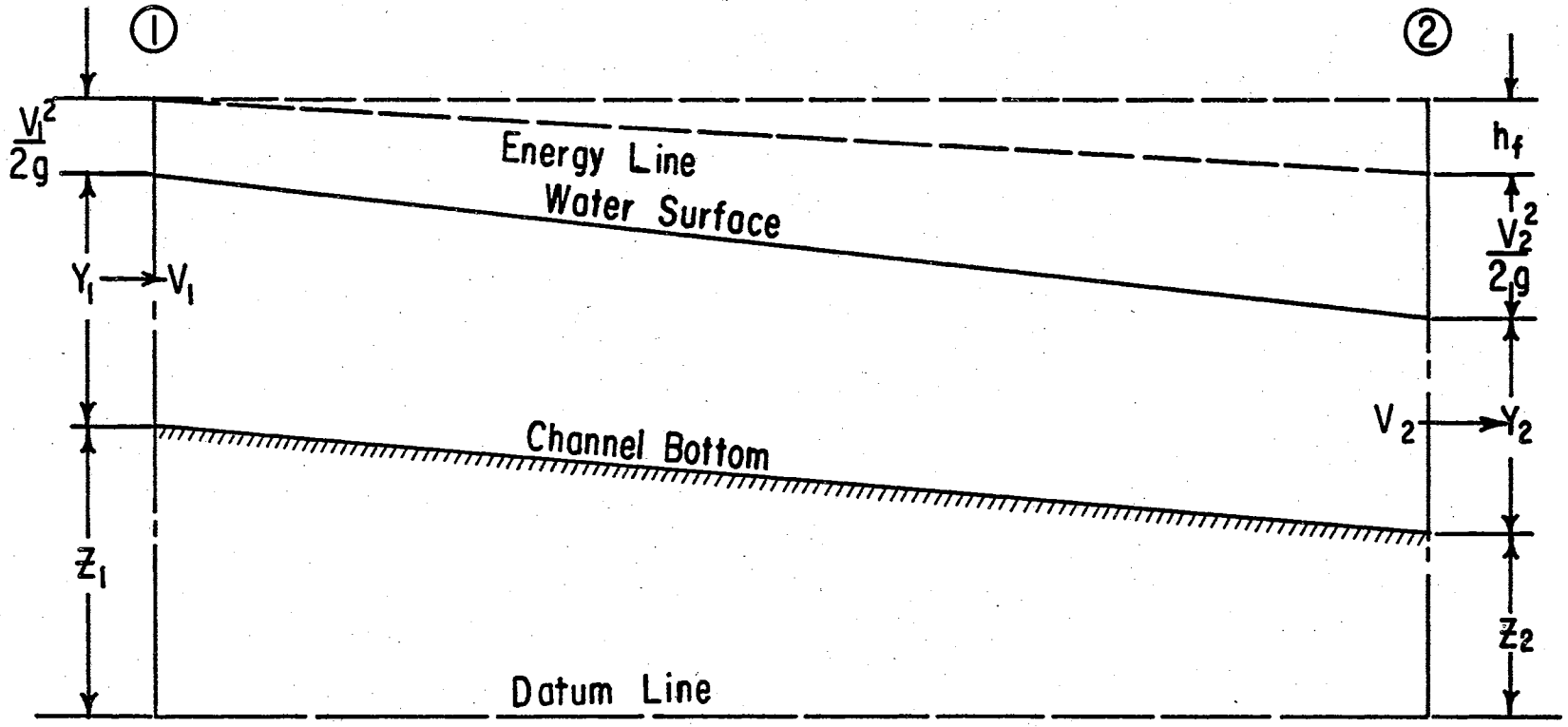

Figure 2. Graphic Description of Total Energy in Open Channel Flow

Combinations of steady, unsteady, and uniform, non-uniform flow can occur.

Steady uniform flow is the basic type of flow treated in open channel hydraulics. In this type of flow the depth does not change both in the reach and time interval under consideration.

Steady non-uniform (varied) flow occurs when the depth at X = C is constant, but depth varies along the reach.

Manning's Equation

The most widely used of all uniform flow formulas for open channel computation is Manning's equation.

Manning, an Irish Engineer, presented the equation in the late 19th century. The equation was later modified to its present form:

$$V = \frac{1.49}{n} R^{2/3} S^{1/2} \qquad (2\text{-}1)$$

Where V is the mean velocity in ft/sec, n is the coefficient of roughness known as Manning's n, R is hydraulic radius in feet, and S is the slope of the energy line.

The practical use and application of Manning's equation depends upon a proper selection of the roughness coefficient n. But the greatest difficulty is the determination of the roughness n. Without experimentation, only an estimate can be made.

n is dependent upon many factors. In a fixed boundary channel made of a homogeneous material, n is dependent upon:

1. Surface roughness. Surface roughness being a function of the size and shape of grains forming the wetted perimeter and producing

a retarding effect on flow.

2. Manning's n is also a function of N_{RE} (Reynold's Number). Generally in a fixed boundary channel n decreases as N_{RE} increases in turbulent flow.

Nevertheless, the Manning equation with constant n is applicable to the fully rough zone of turbulent flow. The Reynolds number is the usual criterion for identifying the fully turbulent regime. For sufficiently high Reynold's number, Manning's n is very nearly constant.

Preliminary investigations and design work are dependent on a reasonable assumption of Manning's n for the material in use. Most texts include tables of Manning's n for various types of channel materials. Design values for smooth metal surfaces range from 0.011. to 0.015. Table I contains values of Manning's n for smooth metal surfaces.

TABLE I

MANNING'S n FOR SMOOTH METAL SURFACES

Author	Description of Surface	Range of n
King (16)	Smooth Metal Flumes	.011-.015
Chow (5)	Smooth Steel Surface	.011-.014
Woodward (28) and Posey	Smoothest Metal Surfaces	.011-.012

Gradually Varied Flow

Gradually varied flow is a form of steady non-uniform flow. It is steady flow where the depth varies gradually along the length of the channel.

According to Chow (5), there are two basic assumptions that most theories developed on gradually varied flow depend on:

> 1. The head loss at a section is the same as for a uniform flow having the velocity and hydraulic radius of the section.
>
> 2. The uniform flow formula may be used to evaluate the energy slope of a gradually varied flow at a given channel section and the corresponding coefficient of roughness developed primarily for uniform flow is applicable to the varied flow.

Gradually varied flow problems can be approached from two methods: The law of conservation of energy and the law of conservation of momentum.

According to Chow (5),

> The inherent distinction between the two principles lies in the fact that energy is a scaler quantity whereas momentum is a vector quantity. Also the energy equation contains a term for internal loss, whereas the momentum equation contains a term for external resistance.

Energy Method

Bernoulli's equation can be applied to gradually varied flow. It is an application of the principle of conservation of energy where the total energy at station 1 is equal to the total energy at station 2 plus friction losses.

Bernoulli's equation written for gradually varied flow is (5):

$$Z_1 + Y_1 + \alpha \frac{V_1^2}{2g} = Z_2 + Y_2 + \alpha \frac{V_2^2}{2g} + h_f \qquad (2\text{-}2)$$

At channel cross sections 1 and 2, Z is the bottom elevation, Y is the depth of water perpendicular to the bottom, α is the coriolis velocity distribution coefficient, V is the mean velocity, and g is the acceleration of gravity.

The dynamic or differential equation of gradually varied flow is derived from the total energy concept. Consider the channel in Figure 3, the total energy head above the datum at the upstream section 1 is:

$$H = Z + d \cos \theta + \alpha \frac{V^2}{2g} \qquad (2\text{-}3)$$

Assume α and θ are constant and taking the bottom of the channel as the X axis and differentiating Equation (2-3) with respect to X gives:

$$\frac{dH}{dX} = \frac{dZ}{dX} + \cos \theta \ \frac{dd}{dX} + \alpha \ \frac{d}{dX} \left(\frac{V^2}{2g} \right)$$

Where $\frac{dH}{dX} = S_f$ is the friction slope and $\frac{dZ}{dX} = S_o$ is the bottom slope. Friction loss dH is always negative (5), so $S_f = \frac{-dH}{dX}$. The bottom slope, negative for a descending bottom is $S_o = \frac{-dZ}{dX}$. Assuming $\cos \theta \approx 1$ and $d \approx Y$, the above equation can be solved for $\frac{dY}{dX}$:

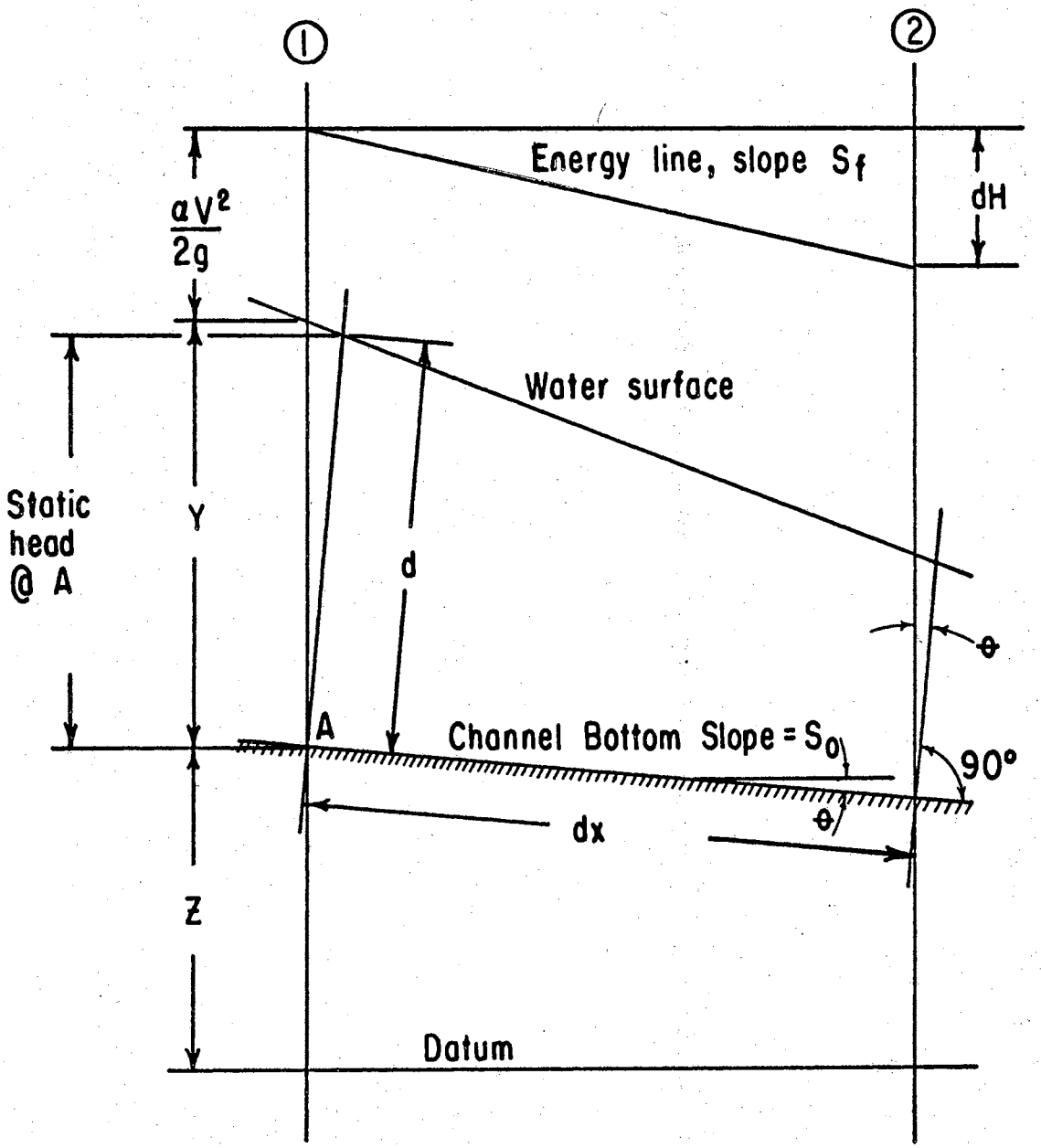

Figure 3. Graphic Illustration of Gradually Varied Flow

$$\frac{dY}{dX} = \frac{S_o - S_f}{1 + \alpha \, d\left(\frac{V^2}{2g}\right) / dY} \qquad (2\text{-}4)$$

Equation (2-4) is the general differential equation of gradually varied flow (5).

Momentum Equation

According to Newton's second law of motion, the change of momentum per unit of time in a body of water flowing in a channel, equals the resultant of all the external forces that are acting on the body.

In an open channel the forces are pressure, gravity, and shear.

The following equation for momentum change can be written between sections 1 and 2 (5).

$$\frac{Qw}{g}(B_2V_2 - B_1V_1) = P_1 - P_2 + W \sin \theta - F_f \qquad (2\text{-}5)$$

Where Q is the discharge in c.f.s., w is the unit weight of water in lbs/ft^3, B is the momentum coefficient, V is the velocity in ft/sec, P_1 and P_2 are the resultant pressures. W is the weight of water enclosed between the sections, and F_f is the total external force of friction and resistance acting along the surface of contact between the water and the channel.

According to Chow(5), the following assumption can be made for gradually varied flow; P_1 and P_2 can be computed by assuming a hydrostatic distribution of pressure.

In a reach of small slope, the following equation can be written from Equation (2-5).

$$z_1 + Y_1 + \frac{B_1 V_1^2}{2g} = z_2 + Y_2 + \frac{B_2 V_2^2}{2g} + h_f^1 \qquad (2\text{-}6)$$

Where h_f^1 is a measure of external head losses due to friction, according to Chow (5), h_f^1 equals h_f even though their definitions are not the same.

Spatially Varied Flow

Spatially varied flow is a form of open channel flow where water is either added to or taken off along the course of flow. There are two types of spatially varied flow:

1. Increasing spatially varied flow, and
2. Decreasing spatially varied flow.

Increasing Spatially Varied Flow

Increasing spatially varied flow occurs when water is added along the course of flow. Practical examples are side-channel spillways in dams, flow in roof gutters, and flow in a vegetated waterway used as a drainage ditch. According to Chow, most hydraulicians apply the momentum principle to problems on increasing spatially varied flow and the energy principle to problems on decreasing spatially varied flow.

Decreasing Spatially Varied Flow

Decreasing spatially varied flow occurs when the flow is gradually diminished along the course of flow. Flow in an irrigation

distribution system is a form of decreasing spatially varied flow where siphon tubes, weirs, or orifice plates are used to take a portion of Q off at certain intervals. Flow in a sprinkler system is also a form of decreasing spatially varied flow.

According to Chow (5), decreasing spatially varied flow is best analyzed by using the energy approach. Below is the derivation of the differential equation for decreasing spatially varied flow derived from the energy equation.

The total energy at a channel section is

$$H = Z + Y + \alpha \frac{Q^2}{2gA^2}$$

differentiating this equation with respect to X and assuming α equals constant

$$\frac{dH}{dX} = \frac{dZ}{dX} + \frac{dY}{dX} + \frac{\alpha}{2g}\left(\frac{2Q}{A^2}\frac{dQ}{dX} - \frac{2Q^2}{A^3}\frac{dA}{dX}\right)$$

where

$$\frac{dH}{dX} = -S_f, \quad \frac{dZ}{dX} = -S_o, \quad \frac{dQ}{dX} = q$$

and

$$\frac{dA}{dX} = \left(\frac{dA}{dY}\right)\left(\frac{dY}{dX}\right) = \frac{TdY}{dX}$$

The above equation becomes

$$\frac{dY}{dX} = \frac{S_o - S_f - \alpha \frac{Qq}{gA^2}}{1 - \alpha \frac{Q^2}{gA^2 D}} \qquad (2\text{-}7)$$

Equation (2-7) is the differential equation for decreasing spatially varied flow. Water surface profiles can be calculated by replacing differentials dX and dY with finite increments ΔX and ΔY.

Decreasing spatially varied flow was first used in the design of lateral spillways. Engels, Coleman, and Smith (5,6) did the first work in this area. Their work was mainly empirical in nature. Engels observed rising water surface profiles while Coleman and Smith observed falling water surface profiles.

Nimmo and DeMarchi (6) were the first to use a theoretical approach. Both of their theories when simplified reduced to Equation (2-7).

DeMarchi made a significant contribution and cleared up some existing problems in previous experimentation. He explained the cause of rising water surface profiles vis a vis the cause of falling water surface profiles.

Rising profiles occurred in subcritical flow and falling profiles occurred in supercritical flow, where the Froude number, Fr equals $V/\sqrt{gD}$, is used to differentiate between subcritical and supercritical flow.

$Fr > 1$ denotes supercritical flow

$Fr < 1$ denotes subcritical flow

Recently several people have done work on decreasing spatially varied flow in irrigation distribution channels where the flow was discharged by siphon tubes, weirs, and submerged tubes.

Mink (19) did work with a concrete trapezoidal irrigation channel with siphon tubes. He found that Manning's n for gradually varied flow does not accurately predict the water surface profile for decreasing spatially varied flow tests.

Both Mink (19) and Sweeten (24) used the same method in calculating an adjusted value of Manning's n for decreasing spatially varied flow which they called $\bar{n}$. Using the Bernoulli energy equation written for spatially varied flow:

$$\frac{V_2^2}{2g} + Y_2 + Z_2 = \frac{V_1^2}{2g} + Y_1 + Z_1 + S_f \Delta X \qquad (2\text{-}8)$$

where the downstream and upstream stations are 1 and 2, respectively, and ΔX is the difference between the two stations. Rearranging the Manning equation and substituting it into Equation (2-8) gives:

$$\frac{Q_2^2}{2gA_2^2} + Y_2 + Z_2 = \frac{Q_1^2}{2gA_1^2} + Y_1 + Z_1 + \frac{Q_2^2 \bar{n}^2 \Delta X}{2.208\, A_{avg}^2 R_{avg}^{1.333}} \qquad (2\text{-}9)$$

where

$$V = \frac{Q}{A}$$

$$A_{avg} = \frac{1}{2}(A_1 + A_2)$$

$$R_{avg} = \frac{1}{2}(R_1 + R_2)$$

This equation can be used to solve for $\bar{n}$ by starting calculations at the downstream end of the irrigation bay where Q = 0 and Z is known, and the water surface elevation, $Y + Z$ is measured. Incrementing Y between successive siphon tubes or stations with Q increasing in an upstream direction will yield a calculated water surface profile. If $\bar{n}$ has not been properly selected the calculated and observed profiles will not agree. The final upstream point can be checked to see if the calculated and observed values concur. If the calculated value over-predicts the observed value $\bar{n}$ must be decreased and if the calculated value underpredicts the observed value $\bar{n}$ must be increased.

Mink and Sweeten found that $\bar{n}$ values were higher than n calculated for gradually varied flow.

Mink (19) also calculated an effective n which he called n_e. The energy equation using the upstream and downstream channel sections of a bay can be written as:

$$\frac{V_i^2}{2g} + Y_i + Z_i = \frac{V_o^2}{2g} + Y_o + Z_o + S_{fe}L \qquad (2\text{-}10)$$

where i and o refer to the upstream and downstream sections.

V_o equals 0, and the effective slope of the energy line between the upstream and downstream section is:

$$S_{fe} = \frac{1}{L}\left[\frac{V_i^2}{2g} + (Y_i + Z_1) - (Y_o + Z_o)\right] \qquad (2\text{-}11)$$

n_e can be calculated by substituting Manning's equation for S_{fe}.

$$n_e = \frac{1.486\ A_i R_i^{2/3}}{Q_i} \left[\frac{1}{L} \left(\frac{Q_i^2}{2gA_i^2} + WS_i - WS_o \right) \right]^{\frac{1}{2}} \qquad (2\text{-}12)$$

Sweeten (24) derived the following relationship between the roughness coefficients $\bar{n}$ and n_e.

$$\bar{n} = \sqrt{3}\ n_e \qquad (2\text{-}13)$$

Sweeten (24) using the same channel as Mink varied siphon tube spacing and siphon tube diameter. He found that hydraulic roughness increases with closer spacing, larger tube diameter, and greater submergence. He also found $\bar{n}$ much better than n from gradually varied flow for calculating and predicting water surface profiles for decreasing spatially varied flow.

Sweeten (24) made a significant contribution in deriving an equation for calculating water surface profiles when the average value of $\bar{n}$ for a channel was known.

According to Sweeten (24) in a horizontal channel velocity head gain and friction head loss contribute to the difference in potential energy. So the change in water surface elevation ΔWS between an upstream station at x equal to 0 and a downstream location at x equal to X can be expressed as:

$$\Delta WS = \Delta h_v - h_f \qquad (2\text{-}14)$$

where velocity head recovery is:

$$\Delta h_v = \frac{V_i^2}{2g} - \frac{V_x^2}{2g} \qquad (2\text{-}15)$$

and the friction losses h_f between the two stations are:

$$h_f = \frac{\bar{n}^2}{2.208\ R^{4/3}} \int_0^X V_x^2\, dx \qquad (2\text{-}16)$$

Where R is the mean hydraulic radius, and the velocity can be expressed as:

$$V_x = V_i\ (1 - \frac{x}{L})$$

By substituting Equation (2-15) and (2-16) into Equation (2-14) and substituting for V_x, the following equation is arrived at:

$$\Delta WS = \frac{V_i^2}{2g}\left(\frac{2X}{L} - \frac{X^2}{L^2}\right) - \frac{\bar{n}^2\, V_i^2}{2.208\ R^{4/3}}\left(X - \frac{X^2}{L} + \frac{X^3}{3L^2}\right) \qquad (2\text{-}17)$$

Equation (2-17) provides a direct solution to solving water surface profiles in a horizontal bay. It also provides a means of solving for $\bar{n}$ when water surface profiles are observed in a horizontal bay.

Sweeten (27) in later research worked out an approach to solving water surface profiles in a two bay situation. The solution is contingent upon an apparent length of bay one. The apparent or virtual channel length L_1' is the length of bay necessary to completely discharge the inflow Q.

$$L_1' = L_s \, Q/Q_{W1} \qquad (2\text{-}18)$$

Where L_s equals orifice or weir spacing

Q equals inflow

Q_{W1} equals flow from one siphon or weir in the upstream bay.

By using L_1 in Equation (2-17), water surface profiles for the upstream bay can be calculated to the point of intersection of the two bays at x equal to L_1. If there is a change in area between the two bays then the water surface elevation downstream is affected by the change in velocity head and the water surface elevation should reflect that change. Calculation of the water surface profile in the second bay proceeds with $L_1 \leq x \leq (L_1 + L_2)$, $L = L_2$, $X = x - L_1$, and Q being the flow into the second bay. Figure 4 shows the decrease in velocity in a two bay situation and also shows the concept of apparent or virtual channel length L_1'.

Sweeten's (27) later research was concerned with the hydraulics of an automated furrow irrigation system with retangular side weir outlets. Sweeten found from the experiments in a single bay mean values of n_e equals 0.0096 and $\bar{n}$ equals 0.01561 and an average value of Manning's n for gradually varied flow was 0.0132. He found that water surface profiles for two bay distributions systems can be calculated using Equation (2-17). Side weir discharge variations ranged from -7.9 to plus 20.0 per cent in the upstream bay.

Discharge from Circular Weirs and Orifices

Greve (10) in 1931 did extensive research on flow from a vertical circular orifice. He conducted tests in several diameters from 0.25

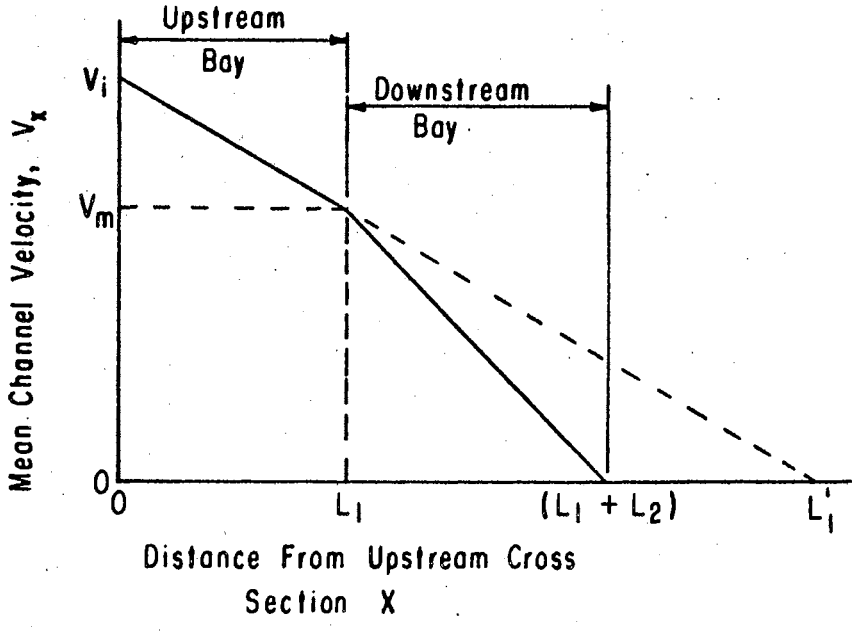

Figure 4. Assumed Decrease in Channel Velocity in a Two Bay Irrigation System With No Change in Area Between Bays

feet to 2.495 feet. Greve used an empirical equation of the form $Q = M(H)^N$ to describe his results. In his experiments a value of M was determined for each diameter and the equation for M was $M = K(D)^L$. Combining these two equations he arrived at a general form $Q = K(D)^L (H)^N$.

Barefoot (3) did work on sloping weirs and orifices. He tested seven diameters from one inch up to eight inches. Barefoot's results contained two significant facts:

1. No significant differences in discharge were detected when different vertical heights from the bottom of the ditch to the bottom of the orifice were used.

2. Barefoot simulated decreasing spatially varied flow conditions in an irrigation ditch where the velocity rates past an orifice would vary. He found no significant differences in discharge for flows from 0.0 up to 2.0 c.f.s.

Barefoot (3) arrived at the following equations:

Equation	Range
$Q = 4.542\ D^{0.549}\ H^{1.953}$	$0.35\text{ ft} < H \quad 0.35\ D$
$Q = 3.710\ D^{0.662}\ H^{1.797}$	$0.35 < H/D < (0.89 - 0.23\ D)$
$Q = 3.450\ D^{1.947}\ (H - 0.35D)^{0.463}$	$H/D > (0.89 - 0.23\ D)$

According to Barefoot (3), there is a good correlation between the discharge determined in his study multiplied by the size of the slope angle and Greve's discharge.

West, working under Barefoot, also did some work on discharge characteristics of circular orifices. His results for vertical

orifices compare favorable with Greve's results, and were used in the hydraulic design in Chapter 3.

CHAPTER III

HYDRAULIC DESIGN

Introduction

An automated cut-back irrigation system was designed utilizing a sheet metal flume as conveyance. The design follows the same principle as the cut-back system designed by Garton (8).

The main operating feature of the cut-back system is its ability to have an initial and then a cut-back flow down the same furrow. This is made possible by dropping the elevation between connecting horizontal bays. The drop between the bays is equal to the difference between heads for initial and cut-back flow.

There are many variables which must be considered in the design of a sheet metal flume for automated cut-back furrow irrigation. Factors which must be considered are; the dimensions of the channel section, the diameter of the orifice, the height of the orifice above the bottom of the channel, orifice spacing, land slope, friction factors n and $\bar{n}$, and the range of initial and cut-back furrow flows.

The first step in the design was to determine the optimum dimensions of the channel section. Next, the optimum height of orifice was determined. Lastly, a design table was constructed for the channel, in which the range of acceptable Q's, slopes, orifice diameters, and initial and cut-back flows are presented.

Section Design

The channel section dimensions are somewhat limited by the size of the material available and the equipment for bending available. Galvanized sheet metal comes in rolls four feet wide and the largest break in the area was ten feet. The maximum wetted perimeter therefore is four feet and each section can be ten feet long.

Beginning with these factors, the first step was to calculate water surface profiles using Sweeten's Equation (2-17) assuming $\bar{n}$ equals 0.0100 and varying.

1. Depth of flow
2. Bottom width
3. Flow, Q
4. Orifice or weir flow (furrow) which in turn fixes the length of channel

The depth of flow was varied from 0.5 feet to 1.1 feet, the bottom width varied from 1.5 feet to 1.7 feet, Q was varied from 1 to 4 c.f.s., furrow flows varied from 10 to 30 g.p.m., and the length varied from 50 to 300 feet.

The object of calculating the profiles was to determine which factors produced the most stable water surface profiles, which in turn would influence the design since the channel slope is horizontal and near horizontal water surface profiles are desired.

From analyzing the results the following conclusions can be made:

1. The greater the depth of flow the more stable the water surface profile.
2. Larger bottom widths have more stable water surface profiles but the differences for different widths are quite small and a deeper

channel is more justified than a wider one.

3. It is best to keep the depth of flow above 0.8 feet.

4. The larger the flow, the less stable are the water surface profiles. Flows from 1 to 2 c.f.s. are best for this size of channel.

A section of bottom width equal to 1.5 feet and depth equal to 1.25 feet was chosen.

Height of Orifice

The next step was to design the height of the bottom of the orifice from the bottom of the channel.

The main consideration in this design is that in a multiple bay operation; e.g., when bay 3 is discharging the initial flow and bay 2 is at cut-back flow, there must be no flow from bay 1. That is, the orifice elevation must be greater than the water surface elevation in all of bay 1, a situation shown in Part C of Figure 1.

This design, for a given field problem, can be solved quite easily. The design would be approached as follows; given a flow Q, field slope, furrow spacing, initial and cut-back furrow flows, and diameter of the orifice (or range of diameters), the set up of the system can be determined; that is, the length of bays and the drop Z between bays. The next step would be to assume an orifice height. When the height of orifice, initial head h_1 and cut-back head h_2 are known, then the water surface elevation at the downstream end of bay 1 can be determined. The difference in the elevation of the water surface between the downstream and upstream ends of bay 1, when it is the cut-off bay, is h_f; i.e., friction loss in the bay h_f can be determined since Q, depth of flow, and length of bay are known.

Now, the allowable difference in the elevation of the water surface at the upper and lower ends of bay 1 is (8):

$$h_f = z_1 + z_2 - h_1 - W \qquad (3\text{-}1)$$

Where h_1 is the initial head in bay 3

z_1 is the drop between bay 1 and bay 2

z_2 is the drop between bay 2 and bay 3

W is the distance the bottom of the orifice must be set above the normal water surface at the upper end of the bay to prevent discharge due to wave action by the wind. W equals 0.01 feet for design purposes.

The actual h_f can be compared to the allowable h_f and in this manner the design can be justified or not.

It was in this manner that a final height for the orifice was determined. That is by considering the design characteristics for varying Q's, slopes, initial and cut-back furrow flows, etc., a final design was arrived at. The final design is a compromise between two factors; friction loss, h_f, and head, h, available for furrow flow. These two factors influence the design in different ways. For example, the higher the orifice the deeper the flow and hence less friction, but less head, h, is available for furrow flow. A low orifice height means low flow depths and hence high friction losses with a greater chance of having the water surface above the orifices in the cut-off bay.

An orifice elevation of 0.75 feet above the bottom of the channel was decided. Limits on values of h_f, free board, and W for wave action

were also set.

$h_f = 0.06$ ft.

$W = 0.01$ ft.

free board $= 0.10$ ft.

h available for furrow discharge $= 0.40$ ft.

Final Design Table

Now that the section dimensions and orifice elevation have been decided, a design table for varying inflows Q, initial and cut-back furrow flows, land slopes, orifice diameter, and orifice spacing can be calculated.

This design table and design nomograph enable a planner to select the system design which best corresponds to a specific field problem within the range of variables presented.

Range of Variables Used in Design

1. Initial and Cut-back Furrow Flows - 6 g.p.m. - 40 g.p.m. This range of flows was selected from past experience and research.
2. Incoming Flow - 1 - 2 c.f.s. system works best for this range of flows.
3. Land Slope - 0.05 per cent - 1.0 per cent slope
4. Furrow Spacing - Various spacings can be used and the nomograph contains a wide range of spacings. The design table is based on 3.33 feet spacing, which was the spacing used for the channel.
5. Orifice Diameter - 1½ inches - 2½ inches most reasonable sizes considering available head and furrow flows.

Table II contains the design table for flows of 1, 1½, and 2 c.f.s. Below is an explanation of the design table.

Explanation of Table II

Column 1 is the cut-back furrow flow in g.p.m., q_2.

Column 2 is the cut-back furrow flow in c.f.s., q_2.

Column 3 is the diameter of orifice.

Column 4 is the head necessary for cut-back flow, h_2.

Column 5 is $2h_2$.

Column 6 is the addition of $2h_2 + (h_f$ + wave action) which equals h_1.

Column 7 is initial furrow flow in c.f.s., q_1.

Column 8 is initial furrow flow in g.p.m., q_1.

Column 9 is Δh equal to $h_1 - h_2$, which is the drop between bays.

Column 10 is the sum of initial and cut-back flows.

Column 11 is the average length of bay equal to $Q/(q_1 + q_2)$ x spacing.

(In this case spacing is 3.33 feet)

Column 12 is the slope S equal to $\Delta h/L$

Column 13 equals Q x S.

TABLE II

HYDRAULIC DESIGN TABLE

1 q_2 gpm	2 q_2 cfs	3 Orif. Diam. inches	4 h_2 ft.	5 $2h_2$ ft.	6 h_1 $h_1=2h_2+0.02$	7 q_1 cfs	8 q_1 gpm	9 Δ $\Delta = h_1-h_2$	10 q_1+q_2 gpm	11 Avg.L ft.	12 Slope $\frac{\Delta}{L}\left(\frac{ft}{ft}\right)$	13 Q x S (cfs)x$\left(\frac{ft}{ft}\right)$
6	0.0133	1 1/2	0.118	0.236	0.256	0.0270	12.11	0.138	18.11	82.51	0.00167	0.00167
		1 3/4	0.114	0.228	0.248	0.0350	15.70	0.134	21.70	68.86	0.00194	0.00194
		2	0.107	0.214	0.234	0.0415	18.62	0.127	24.62	60.70	0.00209	0.00209
		2 1/4	0.098	0.196	0.216	0.0470	21.09	0.118	27.09	55.14	0.00214	0.00214
		2 1/2	0.095	0.190	0.210	0.0500	22.44	0.115	28.44	52.54	0.00218	0.00218
8	0.0178	1 1/2	0.148	0.296	0.316	0.0310	13.91	0.168	21.91	68.19	0.00246	0.00246
		1 3/4	0.143	0.286	0.306	0.0400	17.95	0.163	25.95	57.57	0.00283	0.00283
		2	0.125	0.250	0.270	0.0460	20.64	0.145	28.64	52.18	0.00277	0.00277
		2 1/4	0.117	0.234	0.254	0.0540	24.23	0.137	32.23	46.35	0.00295	0.00295
		2 1/2	0.113	0.226	0.246	0.0630	28.27	0.133	36.27	41.19	0.00322	0.00322
10	0.0223	1 1/2	0.187	0.374	0.394	0.0355	15.93	0.207	25.93	57.60	0.00359	0.00359
		1 3/4	0.150	0.300	0.320	0.0410	18.40	0.170	28.40	52.61	0.00323	0.00323
		2	0.141	0.282	0.302	0.0495	22.21	0.161	32.21	46.38	0.00347	0.00347
		2 1/4	0.132	0.264	0.284	0.0590	26.48	0.152	36.48	40.95	0.00371	0.00371
		2 1/2	0.127	0.254	0.274	0.0690	30.96	0.147	40.96	36.46	0.00403	0.00403
12	0.0267	1 3/4	0.177	0.354	0.374	0.0455	20.42	0.197	32.42	46.08	0.00427	0.00427
		2	0.157	0.314	0.334	0.0530	23.78	0.177	35.78	41.75	0.00423	0.00423
		2 1/4	0.147	0.294	0.314	0.0635	28.50	0.167	40.50	36.89	0.00452	0.00452
		2 1/2	0.143	0.286	0.306	0.0750	33.66	0.163	45.66	32.70	0.00498	0.00498
14	0.0312	2	0.175	0.350	0.370	0.0560	25.13	0.195	39.13	38.19	0.00510	0.00510
		2 1/4	0.160	0.320	0.340	0.0675	30.29	0.180	44.29	33.73	0.00533	0.00533
		2 1/2	0.155	0.310	0.330	0.0800	35.90	0.175	49.90	29.93	0.00584	0.00584
16	0.0356	2	0.195	0.390	0.410	0.0600	26.92	0.215	42.92	34.79	0.00617	0.00617
		2 1/4	0.175	0.350	0.370	0.0710	31.86	0.195	47.86	31.20	0.00625	0.00625
		2 1/2	0.168	0.336	0.356	0.0835	37.47	0.188	53.47	27.93	0.00673	0.00673
18	0.0400	2 1/4	0.190	0.380	0.400	0.0760	34.11	0.210	52.11	28.67	0.00732	0.00732
		2 1/2	0.180	0.360	0.380	0.0880	39.49	0.200	57.49	25.97	0.00770	0.00770

Q = 1.0 cfs

TABLE II (Continued)

1 q_2 gpm	2 q_2 cfs	3 Orif. Diam. inches	4 h_2 ft.	5 $2h_2$ ft.	6 h_1 $h_1=2h_2+0.04$	7 q_1 cfs	8 q_1 gpm	9 Δ $\Delta = h_1-h_2$	10 q_1+q_2 gpm	11 Avg.L ft.	12 Slope $\frac{\Delta}{L}\left(\frac{ft}{ft}\right)$	13 Q x S (cfs)x$\left(\frac{ft}{ft}\right)$
6	0.0133	1 1/2	0.118	0.236	0.276	0.0285	12.79	0.158	18.79	119.31	0.00132	0.00198
		1 3/4	0.114	0.228	0.268	0.0370	16.60	0.154	22.60	99.19	0.00155	0.00232
		2	0.107	0.214	0.254	0.0440	19.74	0.147	25.74	87.09	0.00168	0.00252
		2 1/4	0.098	0.196	0.236	0.0510	22.89	0.138	28.89	77.58	0.00177	0.00264
		2 1/2	0.095	0.190	0.230	0.0590	26.48	0.135	32.48	68.99	0.00195	0.00292
8	0.0178	1 1/2	0.148	0.296	0.336	0.0325	14.58	0.188	22.58	99.26	0.00189	0.00284
		1 3/4	0.143	0.286	0.326	0.0415	18.62	0.183	26.62	84.21	0.002173	0.00303
		2	0.125	0.250	0.290	0.0480	21.54	0.165	29.54	75.89	0.002174	0.00326
		2 1/4	0.117	0.234	0.274	0.0575	25.80	0.157	33.80	66.30	0.00236	0.00354
		2 1/2	0.113	0.226	0.266	0.0670	30.07	0.153	38.07	58.87	0.00259	0.00388
10	0.0223	1 3/4	0.150	0.300	0.340	0.0430	19.29	0.190	29.29	76.52	0.00248	0.00372
		2	0.141	0.282	0.322	0.0515	23.11	0.181	33.11	67.69	0.00267	0.00400
		2 1/4	0.132	0.264	0.304	0.0610	27.37	0.172	37.37	59.97	0.00286	0.00430
		2 1/2	0.127	0.254	0.294	0.0715	32.09	0.167	42.09	53.24	0.00313	0.00470
12	0.0267	1 3/4	0.177	0.354	0.394	0.0470	21.09	0.217	33.09	67.73	0.00320	0.00480
		2	0.157	0.314	0.354	0.0550	24.68	0.197	36.68	61.10	0.00322	0.00482
		2 1/4	0.147	0.294	0.334	0.0633	28.41	0.187	40.41	55.47	0.00337	0.00505
		2 1/2	0.143	0.286	0.326	0.0790	35.45	0.183	47.45	47.21	0.00387	0.00580
14	0.0312	2	0.175	0.350	0.390	0.0580	26.03	0.215	40.03	55.97	0.00384	0.00575
		2 1/4	0.160	0.320	0.360	0.0700	31.41	0.200	45.41	49.35	0.00405	0.00607
		2 1/2	0.155	0.310	0.350	0.0830	37.25	0.195	51.25	43.72	0.00446	0.00670
16	0.0356	2 1/4	0.175	0.350	0.390	0.0740	33.21	0.215	49.21	45.55	0.00472	0.00710
		2 1/2	0.168	0.336	0.376	0.0870	39.04	0.208	55.04	40.72	0.00510	0.00765
18	0.0400	2 1/2	0.180	0.360	0.400	0.0910	40.84	0.220	58.84	38.09	0.00577	0.00862

Q = 1 1/2 cfs

TABLE II (Continued)

1 q_2 gpm	2 q_2 cfs	3 Orif. Diam. inches	4 h_2 ft.	5 $2h_2$ ft.	6 h_1 $h_1=2h_2+0.07$	7 q_1 cfs	8 q_1 gpm	9 ℓ $\ell = h_1-h_2$	10 q_1+q_2 gpm	11 Avg.L ft.	12 Slope $\frac{\ell}{L}\left(\frac{ft}{ft}\right)$	13 Q x S $(cfs)x\left(\frac{ft}{ft}\right)$
6	0.0133	1 1/2	0.118	0.236	0.306	0.305	13.68	0.188	19.68	151.88	0.00123	0.00246
		1 3/4	0.114	0.228	0.298	0.0395	17.72	0.184	23.72	126.00	0.00146	0.00292
		2	0.107	0.214	0.284	0.0475	21.31	0.177	27.31	109.42	0.00161	0.00322
		2 1/4	0.098	0.196	0.266	0.0560	25.13	0.168	31.13	96.00	0.00175	0.00350
		2 1/2	0.095	0.190	0.260	0.0660	29.62	0.165	35.62	83.91	0.00196	0.00392
8	0.0178	1 1/2	0.148	0.296	0.366	0.0340	15.62	0.218	23.62	126.54	0.00172	0.00344
		1 3/4	0.143	0.286	0.356	0.0442	19.83	0.213	27.83	107.39	0.00198	0.00396
		2	0.125	0.250	0.320	0.0515	23.11	0.195	31.11	96.07	0.00202	0.00404
		2 1/4	0.117	0.234	0.304	0.0620	27.82	0.187	35.82	83.44	0.00224	0.00448
		2 1/2	0.113	0.226	0.296	0.0730	32.76	0.183	40.76	73.32	0.00249	0.00498
10	0.0223	1 3/4	0.150	0.300	0.370	0.0455	20.42	0.220	30.42	98.23	0.00223	0.00446
		2	0.141	0.282	0.352	0.0545	24.46	0.211	34.46	86.71	0.00243	0.00486
		2 1/4	0.132	0.264	0.334	0.0665	29.84	0.202	39.84	75.02	0.00269	0.00438
		2 1/2	0.127	0.254	0.324	0.0780	35.00	0.197	45.00	66.40	0.00296	0.00592
12	0.0267	2	0.157	0.314	0.384	0.0575	25.80	0.227	37.80	79.05	0.00287	0.00574
		2 1/4	0.147	0.294	0.364	0.0710	31.86	0.217	43.86	68.13	0.00318	0.00636
		2 1/2	0.143	0.286	0.356	0.0840	37.70	0.213	49.70	60.13	0.00354	0.00708
14	0.0312	2 1/4	0.160	0.320	0.390	0.0740	33.21	0.230	47.21	63.30	0.00363	0.00726
		2 1/2	0.155	0.310	0.380	0.0880	39.49	0.225	53.49	55.87	0.00402	0.00804
16	0.0356	2 1/2	0.168	0.336	0.406	0.0910	40.84	0.238	46.84	63.80	0.00373	0.00746

Q = 2.0 cfs

Figure 5 is a nomograph solution of the hydraulic design Table II. The nomograph can be used to select the optimum size of orifice for various operating conditions. An example is shown on the nomograph in Figure 5 and is also explained below.

Given: Inflow Q = 2.0 c.f.s., field slope S = .0020 ft/ft, spacing = 3.33 ft., and initial furrow flow q_1 = 0.0515 c.f.s. = 23.11 g.p.m.

Solution: One line is drawn from Q x S = .0040 through spacing = 3.33 ft. to the center pivot. A second line is drawn from the center pivot point to 0.0515 c.f.s. initial furrow flow. The intersection on the orifice diameter line is at an orifice diameter = 2.0 in. This is the optimum size of orifice for the system.

Figure 6 is a plot of cut-back furrow flow, q_2, versus initial furrow flow, q_1, for different orifice diameters. The plot gives the combinations of initial and cut-back flows that can be used in design with the inflow Q = 2.0 c.f.s. In the previous example, the initial furrow flow, q_1, is 23.11 g.p.m., and the design cut-back furrow flow, q_2, is 8 g.p.m. as shown in Figure 6.

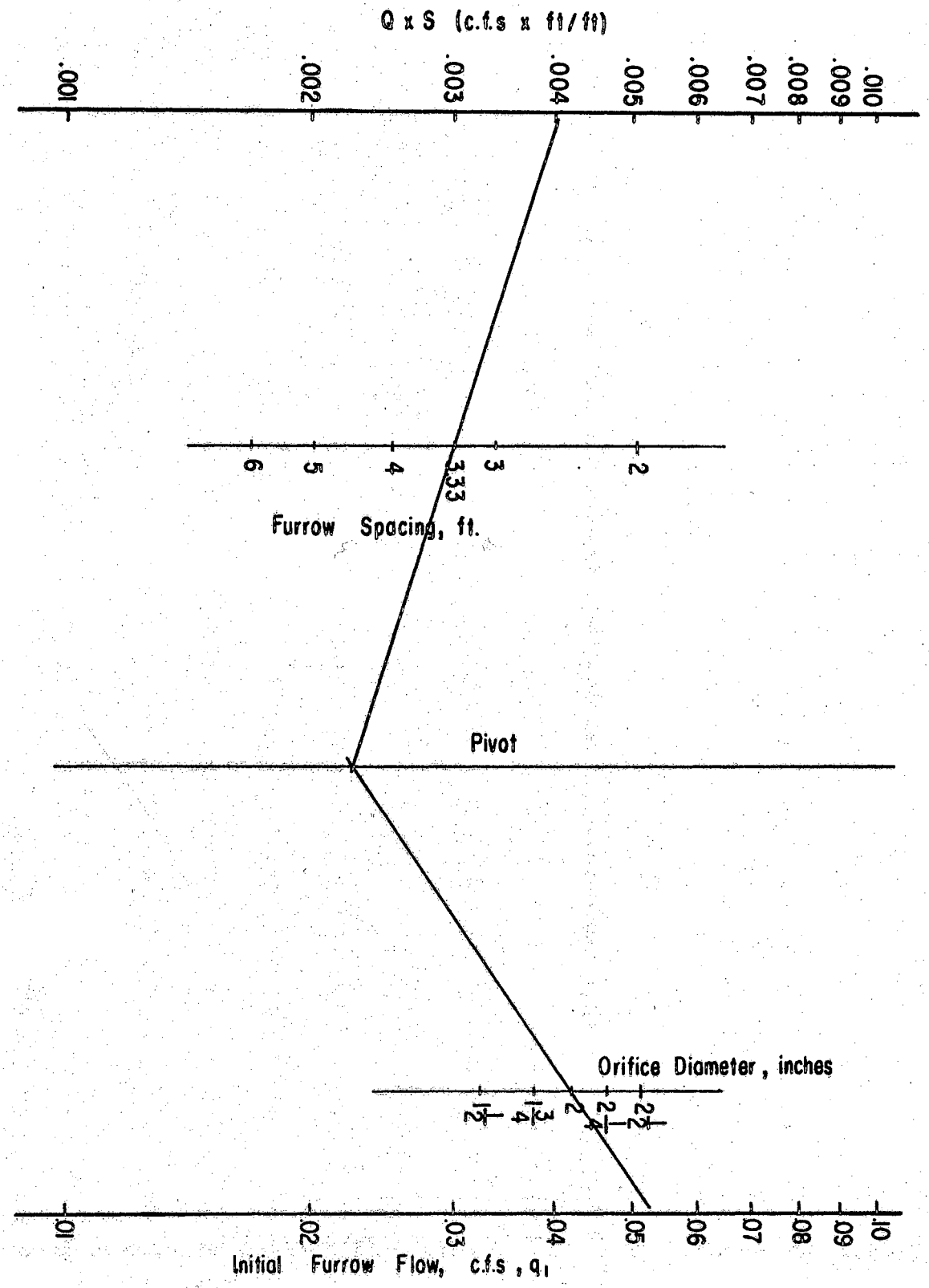

Figure 5. Hydraulic Design Nomograph

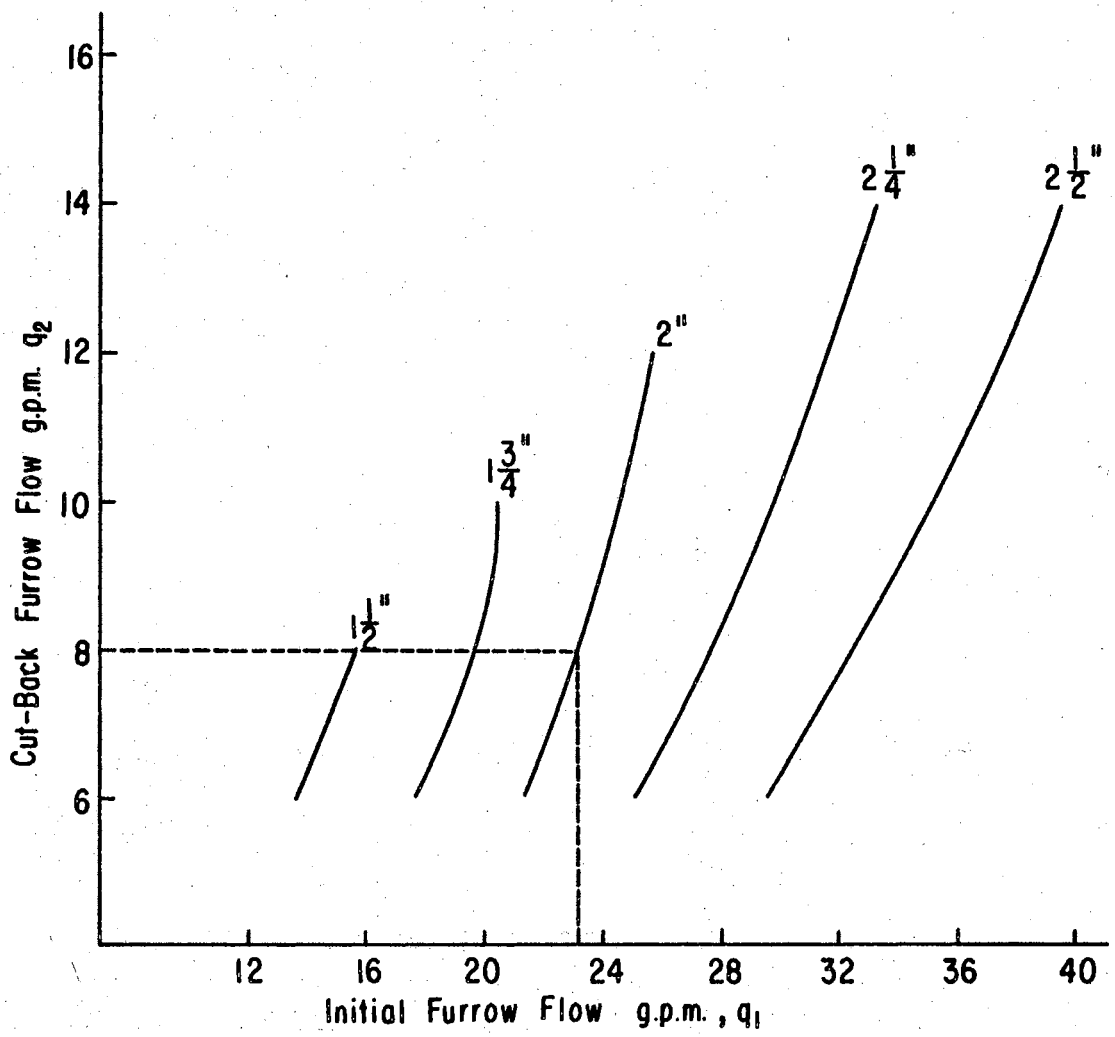

Figure 6. Plot of Acceptable Cut-Back Furrow Flows, q_1, Versus Initial Furrow Flows, q_2, for Different Size Orifices When Inflow $Q \cong 2.0$ c.f.s.

CHAPTER IV

STRUCTURAL DESIGN AND CONSTRUCTION

Introduction

In the preceding chapter a hydraulic design was derived, and the dimensions of the optimum channel section determined. The optimum hydraulic section is a rectangular section open on top 1.5 feet wide, 1.25 feet deep and 10 feet long. The structural investigation and design has this as a starting point. The objective was to design a channel section which is light enough to be easily handled, portable, leak free, easily assembled, and strong enough to withstand permanent bending and buckling. Also it was necessary to support the channel above the ground and to be able to make minor adjustments in the channel elevation in the field.

Preliminary Investigation and Design

Preceding the structural analysis, several types of designs were investigated considering mainly the problem of facilitative assemblage in the field, support of the channel section in the field and leakage. The basic design consists of a structural steel angle frame work as shown in Figure 7. (Note the dimensions of Figure 7 are dimensions for the final design based on structural analysis and testing of various sections; also note that the 1/2 inch by 1/2 inch by 1/8 inch structural angle pieces that run lengthwise on the bottom edges of the

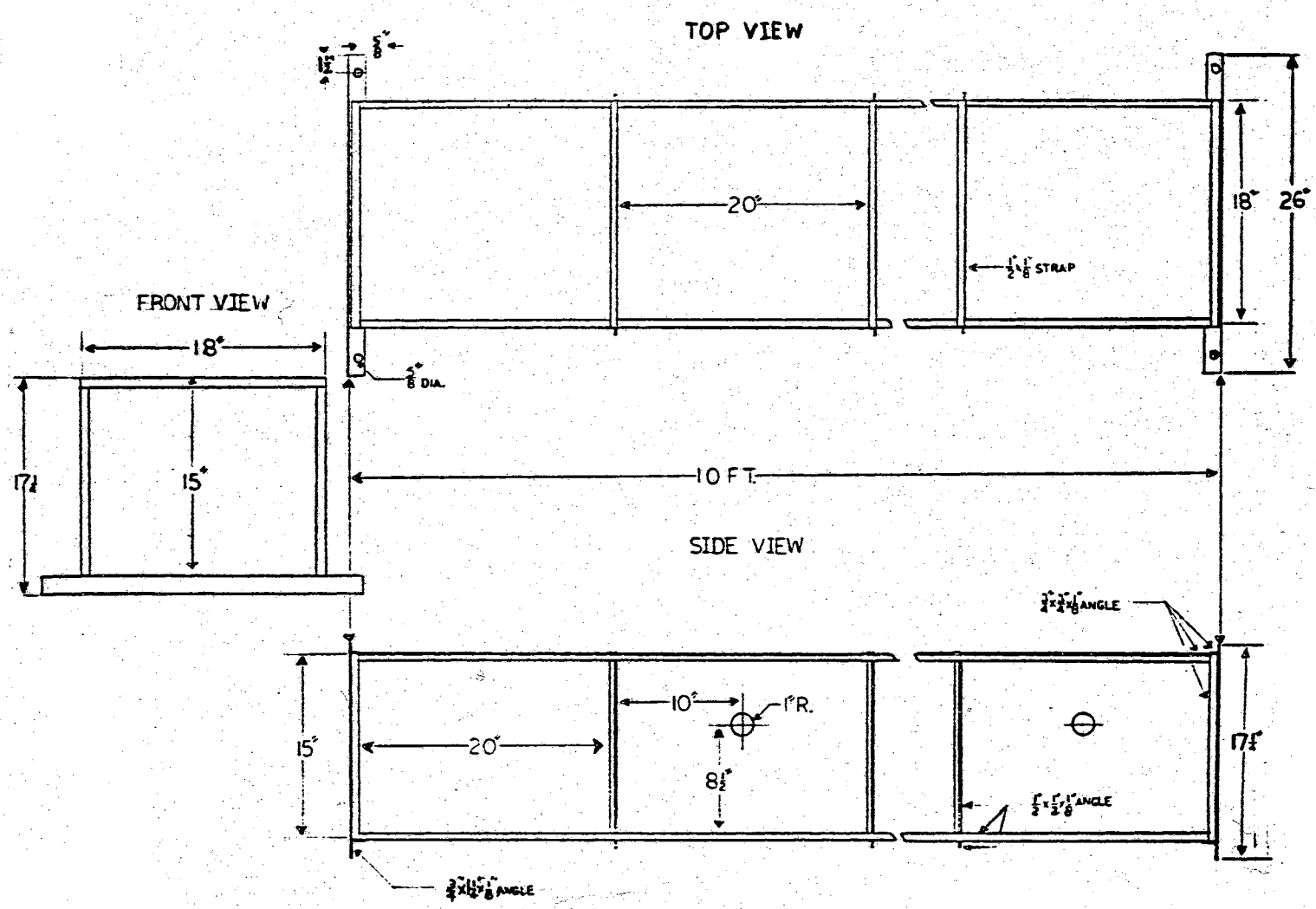

Figure 7. Graphic Illustration of the Structural Steel Angle Framework

sheet metal piece were added to the design strictly to protect the sheet metal from damage when in transport, storage or in the field and were not considered in the preliminary analysis.)

Taking the basic framework selected, several combinations of material designs were considered and investigated theoretically. Three different sizes of structural steel angle frameworks and three sizes of sheet metal were selected. Three frameworks were built for the sizes listed below and six combinations of structural steel angle frameworks and sheet metal sizes were tested by filling the channel section with water. Below is a table of the six combinations used and maximum deflection of the structural steel angle framework and the maximum deflection of the sheet metal. Figure 7 defines the various components of the structural steel angle framework. There are three basic components; (1) rectangular end sections, (2) side and bottom braces, and (3) top and bottom braces.

The various combinations were tested in the Agricultural Engineering Laboratory at Oklahoma State University. Figure 8 shows a section being tested. The final design is the design used in Experiment Number 5 in Table III. It was selected because of its strength and weight advantages. The design proved to withstand full loading and also is relatively light, 8 pounds per linear foot. Figure 7 is a graphic description of the final design.

A basic supporting system was designed as shown in Figure 9. Redwood was used as the base since it responds well to moisture changes. Basic considerations in the design were:

1. The redwood base should have enough bearing area to support the channel in different types of soil;

TABLE III

MAXIMUM DEFLECTIONS FOR SIX DESIGNS TESTED

Experiment Number	Sheet Metal Gage Number	Size of Rectangular End Sections (in.)	Size of Side and Bottom Braces (in.)	Size of Top Braces (in.)	Maximum Deflection of Sheet Metal (in.)	Maximum Deflection of Top Braces (in.)
*1	20	1 x 1 x 3/16	3/4 x 3/4 x 1/8	1 1/4 x 1 1/4 x 3/16	0.240	0.007
*2	24	1 x 1 x 3/16	3/4 x 3/4 x 1/8	1 1/4 x 1 1/4 x 3/16	0.327	0.008
3	20	1 x 1 x 3/16	3/4 x 3/4 x 1/8	1 1/4 x 1 1/4 x 1/8	0.256	0.010
4	24	1 x 1 x 3/16	3/4 x 3/4 x 1/8	1 1/4 x 1 1/4 x 1/8	0.455	0.028
5	24	3/4 x 3/4 x 1/8	1/2 x 1/2 x 1/8	3/4 x 3/4 x 1/8	0.410	0.031
6	26	3/4 x 3/4 x 1/8	1/2 x 1/2 x 1/8	3/4 x 3/4 x 1/8	0.515	0.059

* Note: Only three side and bottom braces were used in these experiments.

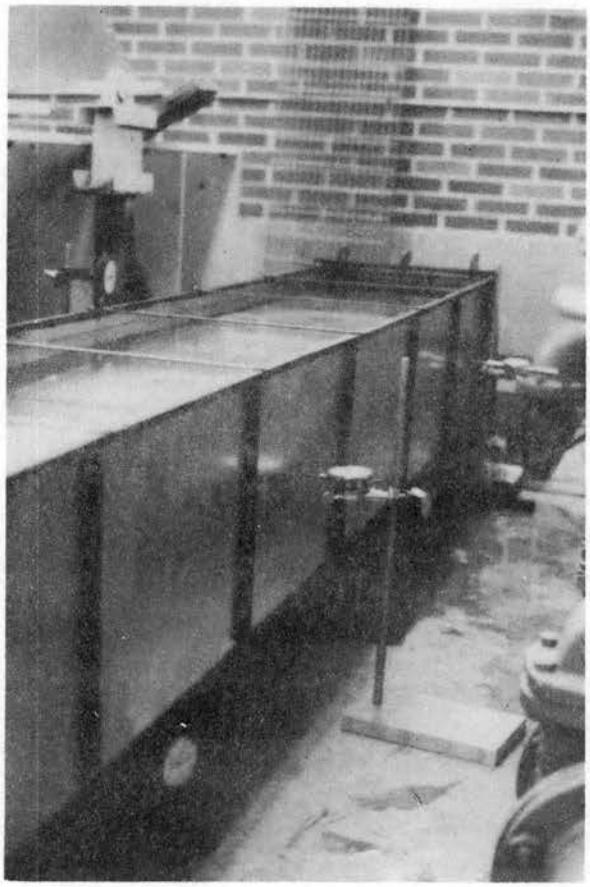

Figure 8. Channel Section Under Load and Deflection Gages

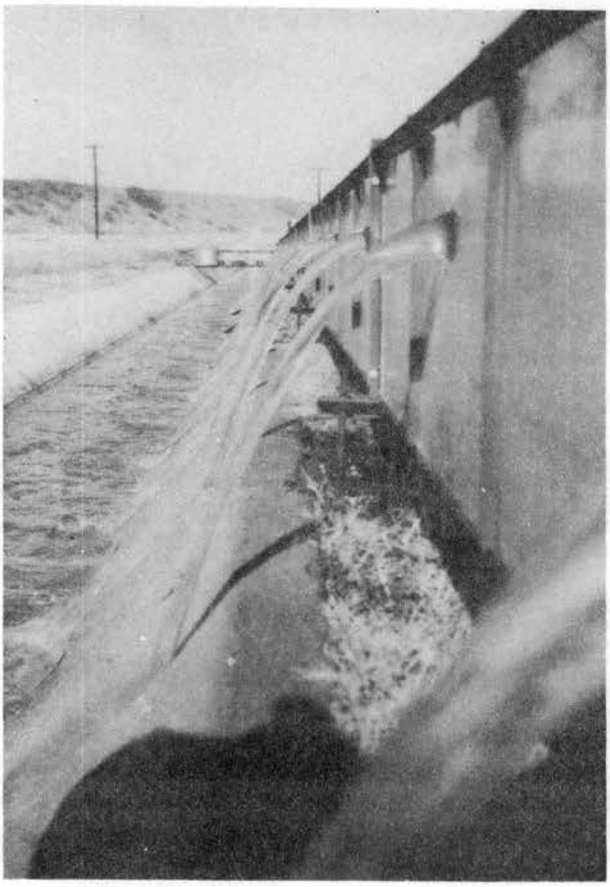

Figure 9. View of Supporting System in the Field

2. The supporting system must be adjustable to adapt to irregularity in field elevation;

3. The column and base must be able to support the load of the channel; and

4. The bearing area of the column base must be large enough so the redwood base can support the load.

Figure 9 shows the stand in operation in the field. A one-half inch diameter steel rod, eight inches long, was used, and a three inch square base one-eighth inch thick was welded to the rod. The two rod-base assemblies were fastened to the redwood base with wood screws.

Construction of the Channel

Figure 10 shows the construction procedure step by step. First, the rectangular end pieces are built with the aid of a jig, Figure 10a. Next, the two rectangular end pieces are placed at opposite ends of a second jig, and the top and bottom braces are welded to the rectangular end pieces, Figure 10b. Next, the side and bottom braces are welded in place, Figure 10c. After the framework is completed, the sheet metal section is placed in the framework and 1/8 inch diameter pop rivets are used to secure the top of the sheet metal section to the top brace, Figure 10d. Pop rivets are also used to secure the sheet metal to the rectangular end pieces.

The problem of leakage occurs at two places; (1) where two channel sections are joined together, and (2) where the sheet metal is joined to the rectangular end pieces. Silicon gel was used as a sealant for the second problem area. Two types of gasket materials were used where the two channel sections are joined together; 1/8 inch

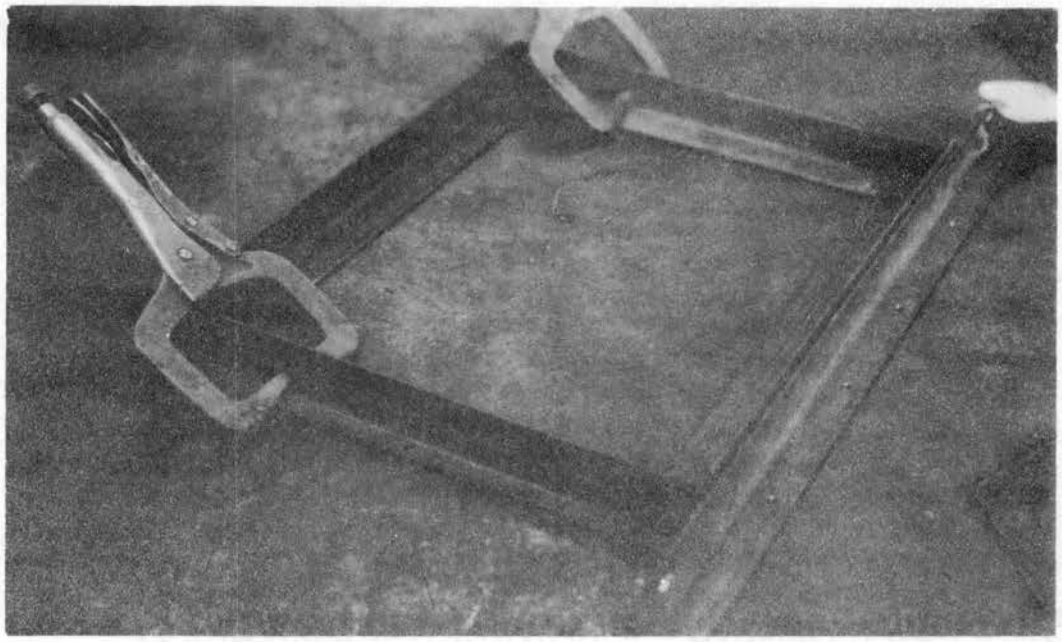

Figure 10a. Construction Procedure - Rectangular End Pieces Being Constructed

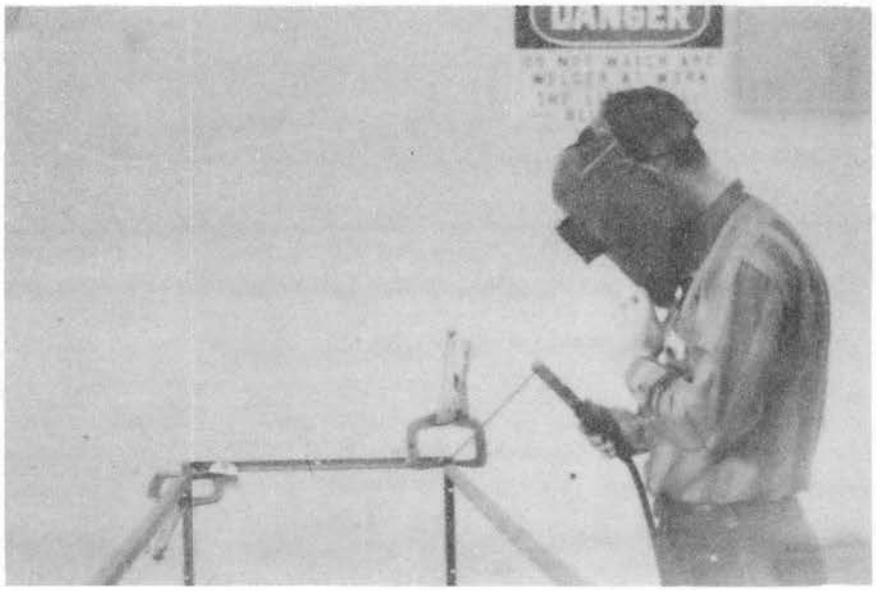

Figure 10b. Top Braces Being Welded to the End Pieces

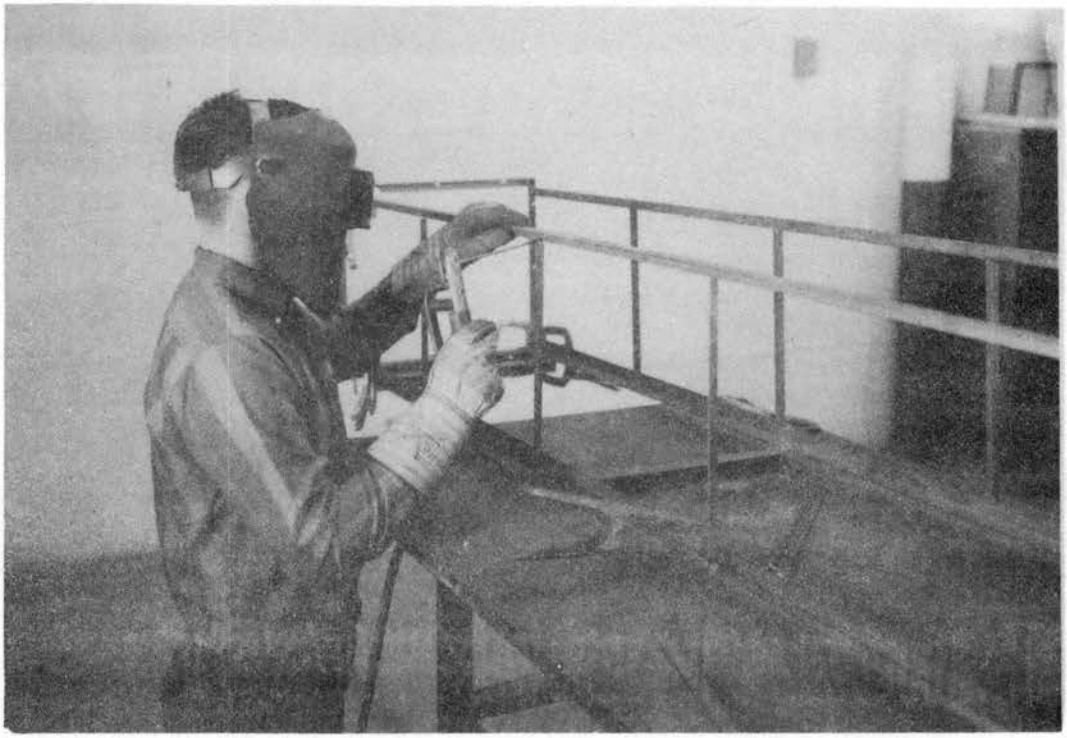

Figure 10c. Side and Bottom Braces Being Welded in Place

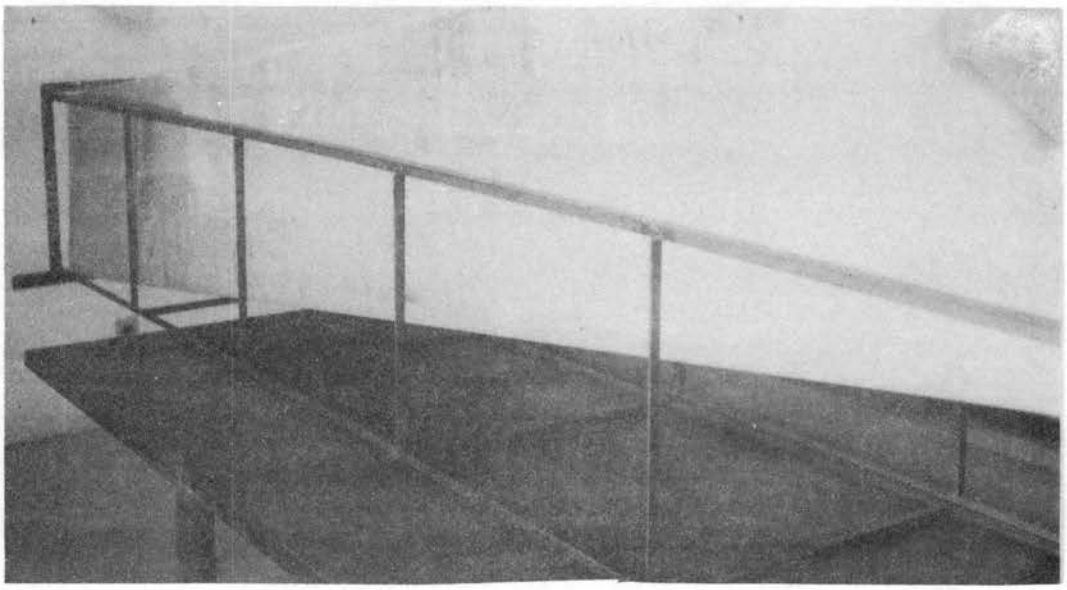

Figure 10d. The Sheet Metal Section Being Installed

thick red rubber and 3/8 inch thick stiff grey rubber. Both were effective in preventing leakage, but the 3/8 inch material worked best, because it allowed more compressibility.

Two time operated check gates were designed and built by Pope (22) and were used in the hydraulic testing.

CHAPTER V

EXPERIMENTAL SETUP AND PROCEDURE

The Channel and Facilities

Facilities at the U.S.D.A. outdoor hydraulic laboratory in Stillwater were utilized for testing. A siphon from Lake Carl Blackwell provided the inflow. The flow was controlled by a 12 inch gate valve and the flow was measured by calibrated orifice plates. A 60 inch water-air manometer was used to measure the differential head across the orifice.

The sheet metal channel was set up next to an existing concrete irrigation channel which facilitated drainage. Refer to Figure 11 for an over-all view of the channel. The total length of the assembled channel was 230 feet, 200 feet of which was the test reach. The first 20 feet of the channel were used to smooth the inflow, and the last 10 feet were used for the outflow. The test reach constituted two 100 foot bays, with a drop between the bays as shown in Figure 12. The drop was located at station 1+20.

At the end of each bay a time operated check gate was located (Figure 13). When wind became a serious problem, light wooden covers were placed on top of the channel.

Measurement

The water surface profile was measured at six stations in each

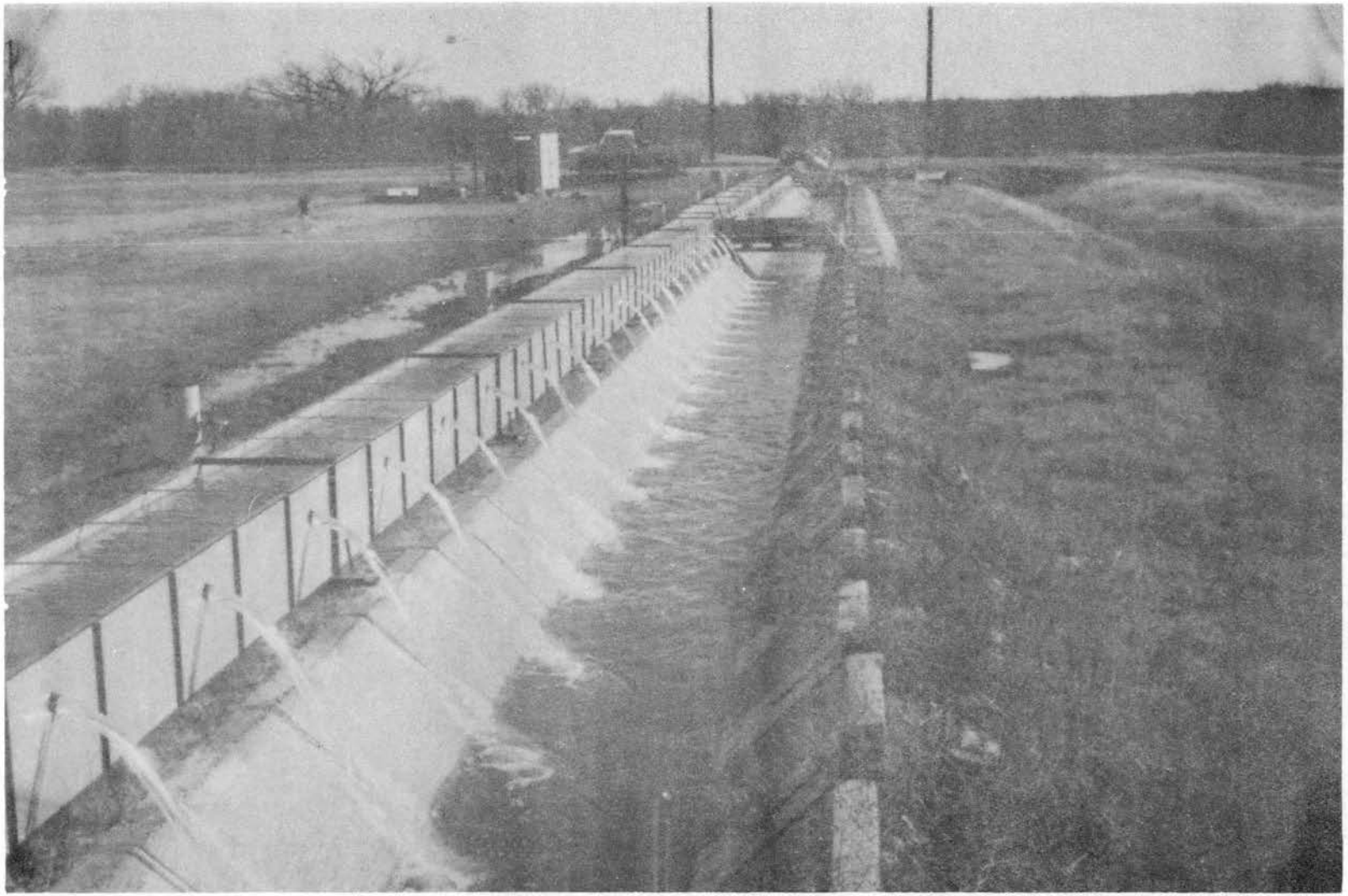

Figure 11. Overall View of the Channel

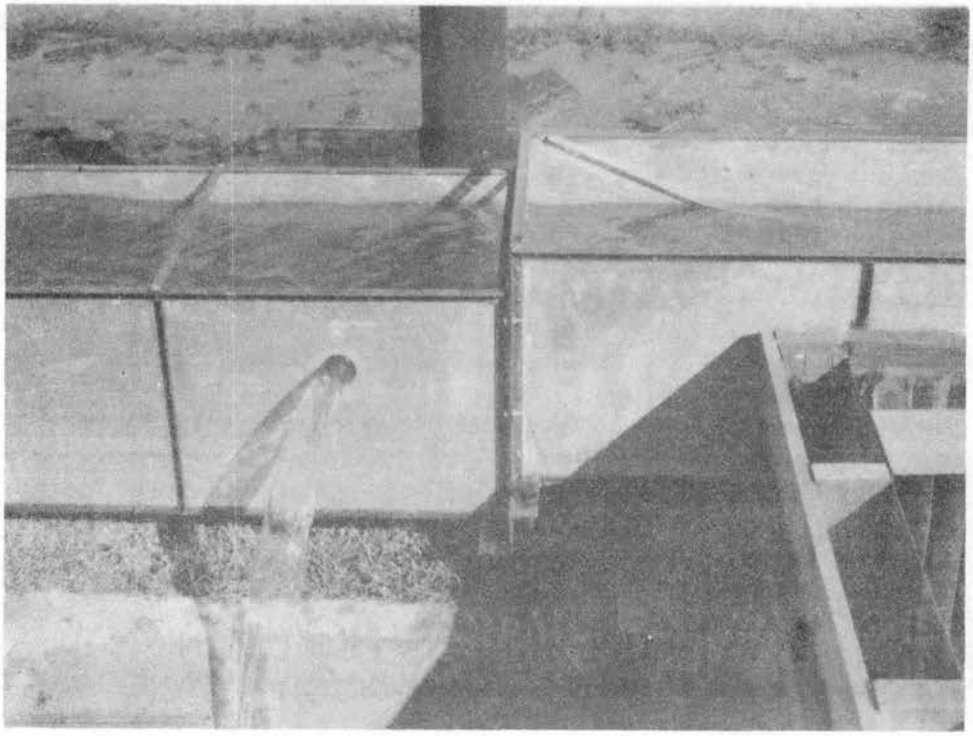

Figure 12. Drop Between Bays

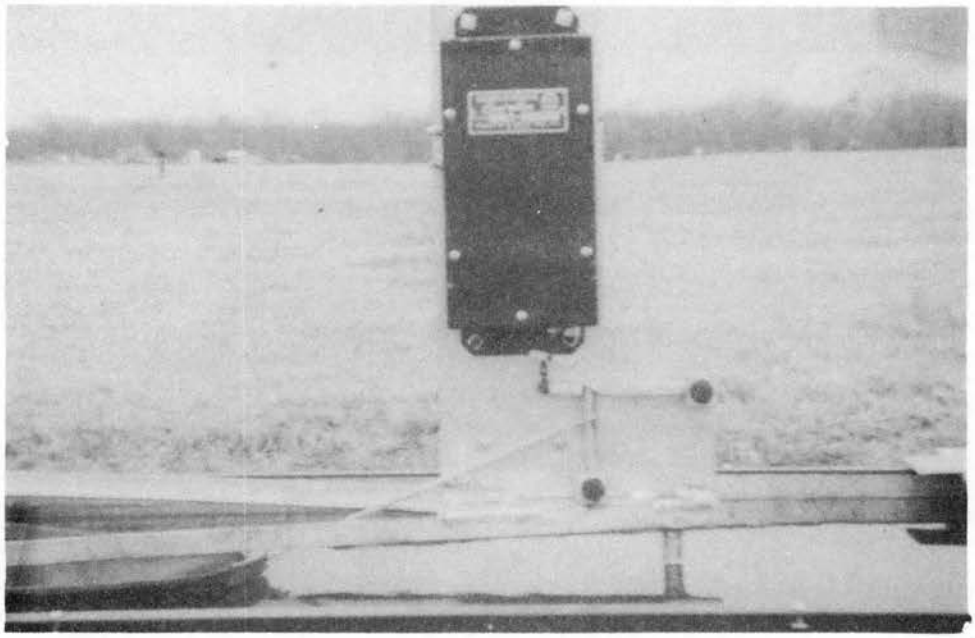

Figure 13. Time Operated Check Gate in Place

bay. Stations were at the following locations; 0+19, 0+39, 0+59, 0+79, 0+99, 1+16, 1+24, 1+41, 1+61, 1+81, 2+01, and 2+21. Two stations, 1+16 and 1+24, were located on either side of the drop between the bays to measure the effect of the drop on the water surface. The water surface elevation at each station was measured at a common stilling well located at station 1+20 (Figure 14). The measurement at the stilling well was done with a two foot point gage readable to 0.001 feet. The piezometric head taps at various stations were connected to the stilling well using 1/8 inch diameter nylon tubing and brass valve fittings were used for the manifold at the stilling well.

A common stilling well facilitated water surface profile readings in that only one reference measurement was needed. The time for readings from distant stations to become stabilized was a problem, and a larger diameter tubing would have facilitated experimentation time.

Three H-Flumes were used to measure the flow from the orifices. During the single bay spatially varied flow tests, the H-Flumes were at the 1st, 18th and 30th orifice starting from the upstream orifice. For the two bay tests the H-Flume at the 18th orifice was moved to the last orifice in bay 2. Figure 15 shows an H-Flume setup for measurement.

Experimental Testing Procedure

Three distinct types of tests were run: gradually varied flow, single bay spatially varied flow, and two bay spatially varied flow tests. Basically the same testing procedure was used for gradually varied flow and spatially varied flow tests.

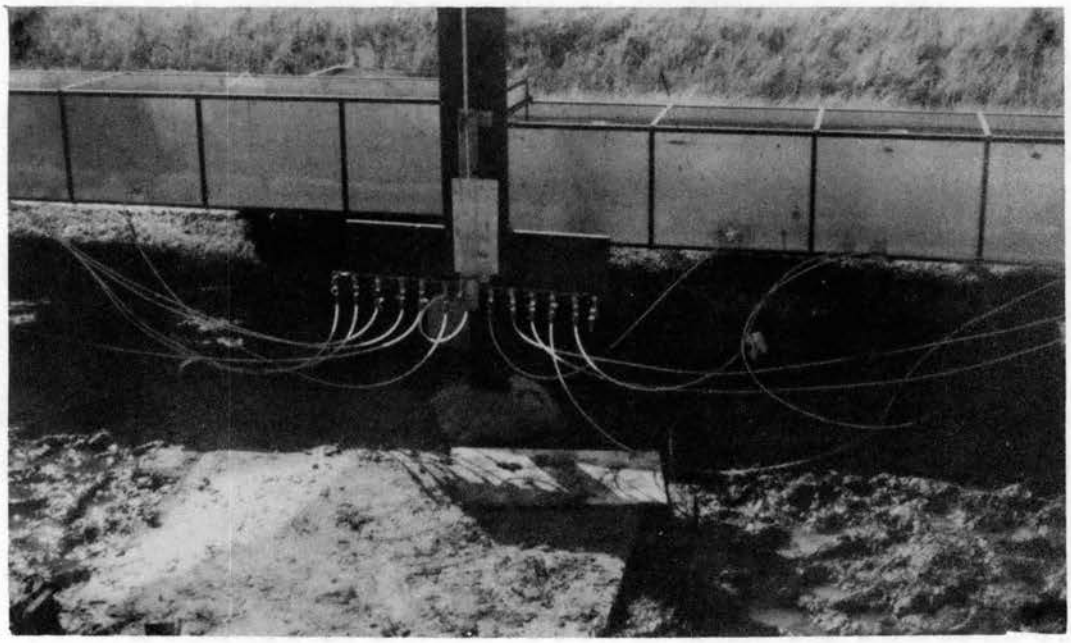

Figure 14. Common Stilling Well Used to Measure Water Surface Elevation

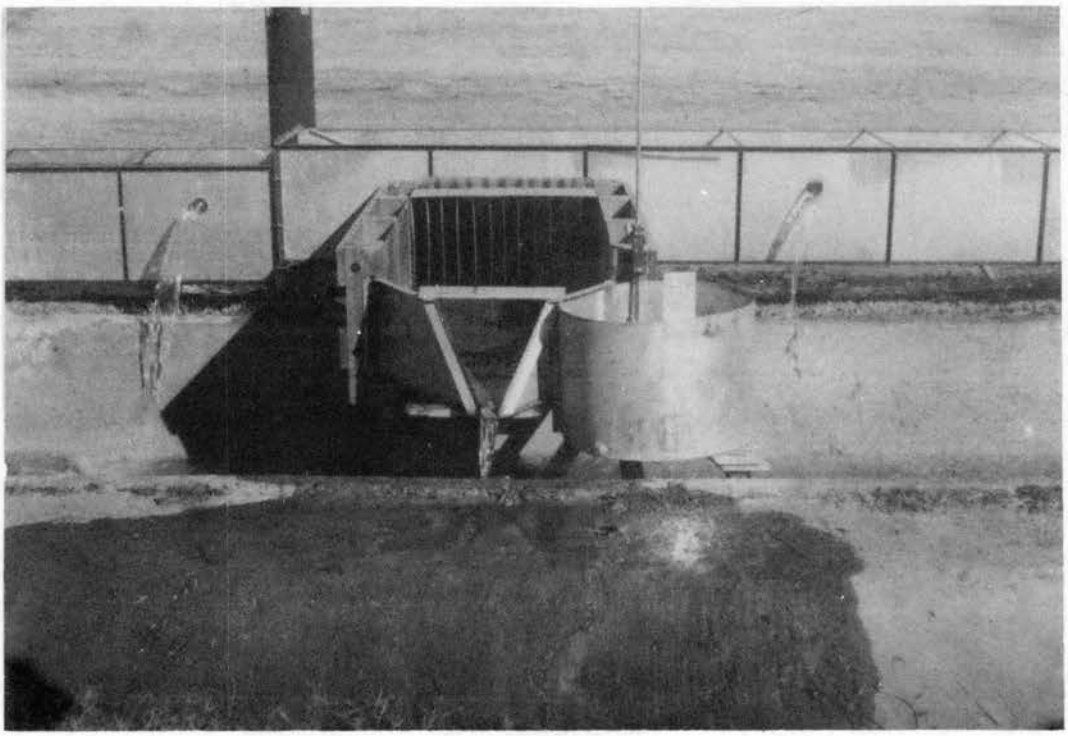

Figure 15. Overall View of H-Flume in Operation

Inflow was initiated and adjusted to the desired flow rate by use of the gate valve and manometer. Flow took on the average, about ten minutes to completely stabilize after which the taking of measurements began.

Inflow through the orifice plate was measured by two variables, the differential head read by the manometer and the water temperature. Observations of the differential head were recorded for each experiment and the average reading was used.

For gradually varied flow, and single bay decreasing spatially varied flow tests, the water surface elevations were measured at the first six stations. For the two bay decreasing spatially varied flow tests the water surface elevations were measured at all twelve stations.

The three H-Flumes were read several times during a test run and an average value at each H-Flume was used.

Finally, at each of the stations where the water surface elevation was measured, the bottom elevation and the elevation of the orifice was also measured.

Reference Procedure

Sweeten's (24) system for referencing gage zeros was used, below is an outline of his method.

A gage zero, determined for a given point gage mounted inside a given gage well, was the elevation of the point gage tip when the zero mark on the point gage shaft coincided with the zero mark on the vernier scale. Surveying with the level and point gage constituted one method of measuring point gage zeros, and this method consisted of

the following steps:

1. With the point gage tip resting on a known elevation (bench mark or previous brass plug) a reading was taken where the line of sight of the instrument crosshair intersected the vertical point gage shaft. This backsight subtracted from the known elevation produced rod zero for the instrument setup. Analogous to height of instrument in conventional surveying, rod zero is defined as the elevation of the point gage tip that would occur if the horizontal instrument crosshair were reading 0.000 feet on the point gage shaft. Hence;

Rod Zero = (Elevation of Bench Mark)-
(Backsight on Point Gage)

2. After moving the point gage to a gage well bracket, a convenient foresight; e.g., 1.000 foot, was established and the vernier scale was read. Subtracting the gage reading from the foresight produced the distance between the crosshair elevation and the vernier zero mark.

3. The remainder obtained in Step 2 was subtracted from the rod zero and the resulting elevation was the gage zero for the station.

Steps 2 and 3 can be expressed as

Gage Zero = Rod Zero - (Foresight - Gage Reading)

CHAPTER VI

ANALYSIS AND DISCUSSION OF RESULTS

Introduction

Gradually varied flow and decreasing spatially varied flow tests were conducted. The objective of the gradually varied flow tests was to determine hydraulic roughness coefficients for various depths and rates of flow. After the gradually varied flow tests were run, orifices were cut and decreasing spatially varied flow tests were started.

Decreasing spatially varied flow tests were run in one bay and two bays. The objectives of the tests were to determine: (1) hydraulic roughness coefficients $\bar{n}$ and n_e; (2) water surface profiles; and (3) weir and orifice discharge uniformity. Weir and orifice discharge was calibrated by the H-Flumes and the orifice plates in the line during the tests.

Gradually Varied Flow Tests

Several gradually varied flow tests were conducted to determine the hydraulic roughness of the channel. A series of tests were designed with three depths of flow for three selected flow rates. A few random tests were also run.

Equation (2-2) was used to solve for the hydraulic roughness n. By assuming $\alpha = 1$, and solving for S_f, Equation (2-2) becomes:

$$S_f = \frac{1}{L}\left[WS_1 - WS_2 + z_1 - z_2 + \frac{Q^2}{2g}\left(\frac{1}{A_1^2} - \frac{1}{A_2^2}\right)\right] \qquad (6\text{-}1)$$

S_f which is the slope of the energy line, can be substituted into Manning's equation (2-1), and Manning's n can be determined

$$n = \frac{1.486\ R^{2/3} S_f^{1/2}}{V} \qquad (6\text{-}2)$$

A computer program was written so that Equation (6-1) could be solved from station to station through the test reach, and an average value of Manning's n was computed for the reach. The test reach was 80 feet long and was from station 0 + 40 to station 1 + 20.

Table IV presents the results of the eleven gradually varied flow tests. Figure 16 is a log-log plot of Manning's n versus VR. VR is the average value of velocity times hydraulic radius for the reach under consideration. The following third degree polynomial equation relates the data with a correlation coefficient $r = .782$ and a standard deviation $s = 0.000214$: $n = 0.01213 - 0.01047\ VR + 0.0154\ VR^2 - 0.0088\ VR^3$. The average value of Manning's n is $n = 0.0096$.

Decreasing Spatially Varied Flow Tests

Several one bay and two bay decreasing spatially varied flow tests were conducted. The objectives of these tests were to find hydraulic roughness coefficient $\bar{n}$, and n_e, to observe water surface profiles, and to determine discharge uniformity.

TABLE IV

HYDRAULIC ROUGHNESS n FOR GRADUALLY VARIED FLOW TESTS

Experiment Number	Q (c.f.s.)	Depth (ft.)	VR	Manning's n
1	1.007	0.578	0.38317	0.01022
2	1.010	0.417	0.45306	0.00963
3	1.035	0.407	0.46316	0.00964
4	1.0499	0.718	0.3584	0.00975
5	1.262	0.467	0.5455	0.00931
6	1.503	0.782	0.4921	0.0100
7	1.527	1.062	0.4223	0.00976
8	1.562	0.529	0.6402	0.00938
9	1.771	0.539	0.7184	0.00924
10	2.008	0.602	0.7844	0.00914
11	2.022	0.778	0.6708	0.00961

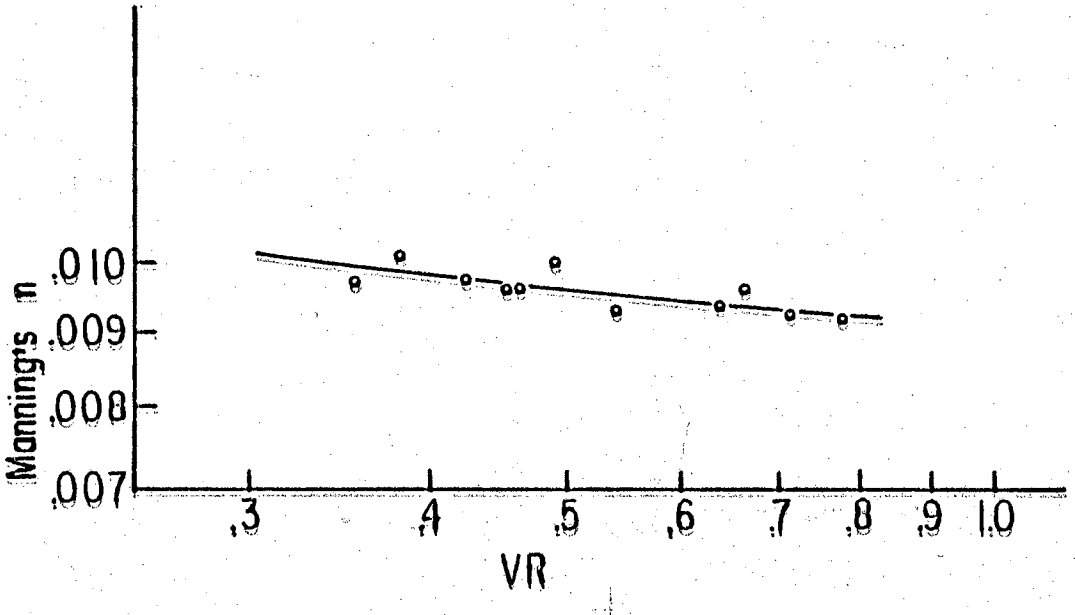

Figure 16. Manning's n Versus VR for Gradually Varied Flow Tests

$\bar{n}$ was calculated utilizing Equation (2-17)

$$\Delta WS = \frac{V_i^2}{2g}\left(\frac{2X}{L} - \frac{X^2}{L^2}\right) - \frac{\bar{n}^2 V_i^2}{2.208\ R_i^{4/3}}\left(X - \frac{X^2}{L} + \frac{X^3}{3L^2}\right) \qquad (2\text{-}17)$$

which, when X = L, reduces to

$$\Delta WS = \frac{V_i^2}{2g} - \frac{\bar{n}^2 V_i^2\ L}{6.624\ R_i^{4/3}} \qquad (6\text{-}3)$$

Equation (6-3) can easily be solved for $\bar{n}$ since V_i, ΔWS, R_i, and L are all known, where V_i is the entering velocity at the start of the test reach in ft/sec, ΔWS is the change in water surface elevation between the upstream and downstream end of the bay in feet, R_i is the hydraulic radius at the start of the test reach in feet, and L is the length of the bay in feet.

The effective roughness coefficient n_e was calculated using Equation (2-12)

$$n_e = \frac{1.486\ A_i\ R_i^{2/3}}{Q_i}\left[\frac{1}{L}\left(\frac{Q_i^2}{2gA_i^2} + WS_i - WS_o\right)\right]^{\frac{1}{2}} \qquad (2\text{-}12)$$

where i and o refer to the upstream and downstream channel sections, respectively, and $V_o = 0$.

Equation (2-12) in effect solves for a roughness coefficient n_e which defines the mean energy slope between the upstream and downstream ends of an irrigation bay.

The hydraulic roughness coefficients $\bar{n}$ and n_e for all single bay tests are listed in Table V. Average values of $\bar{n} = 0.0126$ and $n_e = .00730$ were found.

For the two bay tests a different condition was found in the cut-back bay. Entering flows were quite high, but the depths of flow were quite low; e.g., .865 to .910 feet since it was the cut-back bay. High flows and low depths caused high velocities and, consequently, high values of VR (up to .775) compared to a maximum value of VR = .44 for the single bay tests. These conditions resulted in lower values of $\bar{n}$ and an average value of $\bar{n} = .01065$ was found necessary for design purposes. $\bar{n} = .0126$ was applied to the initial flow bay and $\bar{n} = .01065$ was applied to the cut-back flow bay.

The hydraulic roughness coefficients $\bar{n}$ for the cut-back bay and $\bar{n}$ and n_e for the initial flow bay are listed in Table V, along with the values $\bar{n}$ and n_e for single bay tests. Figure 17 is a log-log plot of $\bar{n}$ versus VR for the decreasing spatially varied flow tests. Values of $\bar{n}$ for both the single bay tests and two bay tests are plotted in Figure 17. A linear regression run in log-log space gave the following equation:

$$\bar{n} = 0.00952\ VR^{-0.26284}$$

with a correlation coefficient $r = 0.88525$ and a standard deviation $s = 0.02172$.

A ratio of $\bar{n}/n_{gvf}$ was computed for single bay tests and compared to Sweeten's (24, 25) values for similar single bay tests using siphon tubes and weir plates. The following value of $\bar{n}/n_{gvf} = 0.0126/0.0096 = 1.31$ was arrived at for the single bay tests for the sheet

TABLE V

HYDRAULIC ROUGHNESS, $\bar{n}$ and n_e FOR SINGLE AND TWO BAY DECREASING SPATIALLY VARIED FLOW TESTS

Single Bay Tests

Experiment Number	Q	Upstream Depth	Upstream VR	WS	$\bar{n}$	n_e
1	0.5381	0.860	0.1664	0.002	0.0087	0.0050
2	0.7217	0.887	0.2200	0.0015	0.0144	0.0083
3	0.7800	0.890	0.2378	0.002	0.0139	0.0080
4	0.8722	0.912	0.2624	0.003	0.0129	0.0074
5	0.9213	0.9115	0.2772	0.003	0.0135	0.0078
6	1.0045	0.923	0.3002	0.0065	0.0082	0.0047
7	1.1122	0.941	0.3289	0.0045	0.0131	0.0076
8	1.2234	0.964	0.3569	0.005	0.0132	0.00766
9	1.3009	0.985	0.3749	0.006	0.0129	0.0074
10	1.3996	1.00	0.3978	0.0065	0.0131	0.0076
11	1.3996	1.0115	0.3907	0.0085	0.0109	0.0063
12	1.5219	1.0385	0.4255	0.009	0.0116	0.0067
13	1.5795	1.050	0.4387	0.007	0.0129	0.0079

Two Bay Tests

Cut-Back Flow Bay

1	1.95	0.863	0.60	0.0145	0.00989	
2	2.089	0.8805	0.64	0.013	0.01021	
3	2.23	0.890	0.68	0.011	0.01016	
4	2.318	0.904	0.71	0.010	0.01045	
5	2.60	0.9315	0.775	0.0093	0.01083	
6	2.0174	0.894	0.61	0.0107	0.01094	
7	2.1493	0.906	0.65	0.0075	0.01070	
8	2.2668	0.925	0.68	0.0055	0.01081	

Two Bay Tests

Initial Flow Bay

1	1.95	1.043	0.4226	0.009	0.0114	0.0066
2	2.089	1.062	0.4353	0.010	0.0109	0.0063
3	2.23	1.070	0.4371	0.0075	0.0133	0.0077
4	2.318	1.076	0.4412	0.009	0.0120	0.0070
5	2.60	1.100	0.4514	0.010	0.0114	0.0066
6	2.0174	1.103	0.3777	0.0075	0.0120	0.0069
7	2.1493	1.120	0.3780	0.007	0.0127	0.0073
8	2.2668	1.1255	0.3782	0.006	0.0142	0.0082

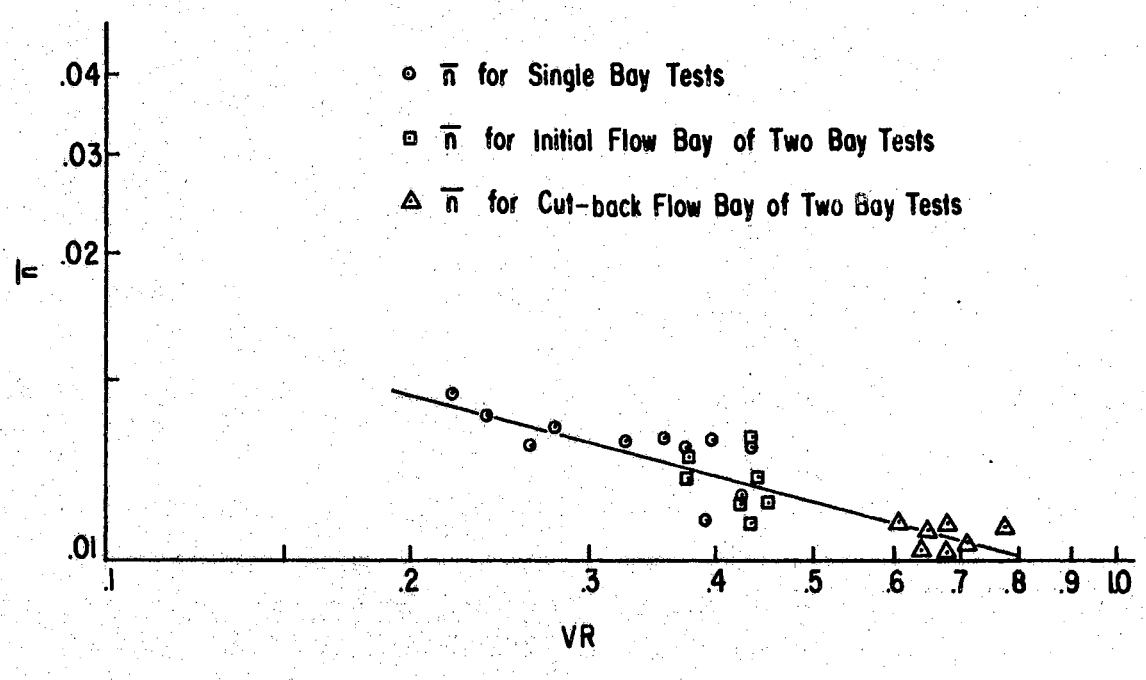

Figure 17. $\bar{n}$ Versus VR for Decreasing Spatially Varied Flow Tests

metal flume as compared to Sweeten's values of $\bar{n}/h_{gvf} = 1.25, 1.28$ for the weir plate and siphon tube tests, respectively.

Analysis of Error in n_e

Some values of $\bar{n}$ and n_e seemed either unusually large or small. Several factors were thought to be the cause of this, one being the inability to read water surface elevations in increments less than 0.001 feet.

Sweeten (25) used a method in similar work to analyze such errors. Equation (2-12) for n_e can be rewritten as:

$$n_e = \frac{1.486}{V_i} R_i^{2/3} \left(\frac{h_f}{L}\right)^{\frac{1}{2}} \tag{6-4}$$

where h_f = loss of energy head, feet.

L = length of the irrigation bay in feet; and the other terms as previously defined.

According to Sweeten (25), using the logarithmic derivitive "Worst Case" method, the expected error n_e was:

$$\frac{\Delta n_e}{n_e} = \frac{\Delta V_i}{V_i} + \frac{2}{3} \frac{\Delta R_i}{R_i} + \frac{1}{2} \frac{\Delta h_f}{h_f} + \frac{1}{2} \frac{\Delta L}{L} \tag{6-5}$$

Neglecting all sources of error except the head loss measurements results in:

$$\frac{\Delta n_e}{n_e} = \frac{1}{2} \frac{\Delta h_f}{h_f} \tag{6-6}$$

where $h_f = \frac{V_i^2}{2g} + WS_i - WS_o$.

Neglecting errors in velocity V_i, the error in measuring the head loss was $h_f = (WS_i - WS_o)$. Values of Δh_f equal $\pm$ .001, and $\pm$ .002 feet were assumed, and the departures Δn_e from the mean effective roughness value of 0.0073 were computed from Equation (6-6) using selected magnitudes of h_f and VR. Values of n_e versus VR for the single bay tests were plotted in Figure 18, and the tolerance bands of $\pm$ .001 and $\pm$ .002 were plotted. One value of n_e was found to lie outside the .002 bands and three values lie outside the .001 bands.

Weir and Orifice Calibration

While one bay and two bay spatially varied flow tests were being run, orifices in both bays were being calibrated by use of three H-Flumes. During the one bay tests, starting from the upstream end of bay 1, orifices 1, 18, and 30 were calibrated. For the two bay tests orifices 1, 30, and 60 were calibrated. The idea was to calibrate orifices at different positions along the bays to study if velocity rates past the orifice had any effect on discharge characteristics. The average diameter of the orifice is 2.01 inches.

Certain problems were encountered in calibrating the orifices. From the recorded flow in the H-Flume and the measured head, h, above the bottom of the orifice, a head, h, versus flow, q, curve was plotted for both weir and orifice flow. This calibration curve showed greater flows for the same head when compared to Barefoot's calibration curve for a 2.0 inch orifice tested under similar flow conditions in the laboratory. Further investigation showed that measured inflow versus measured outflow did not coincide and for all

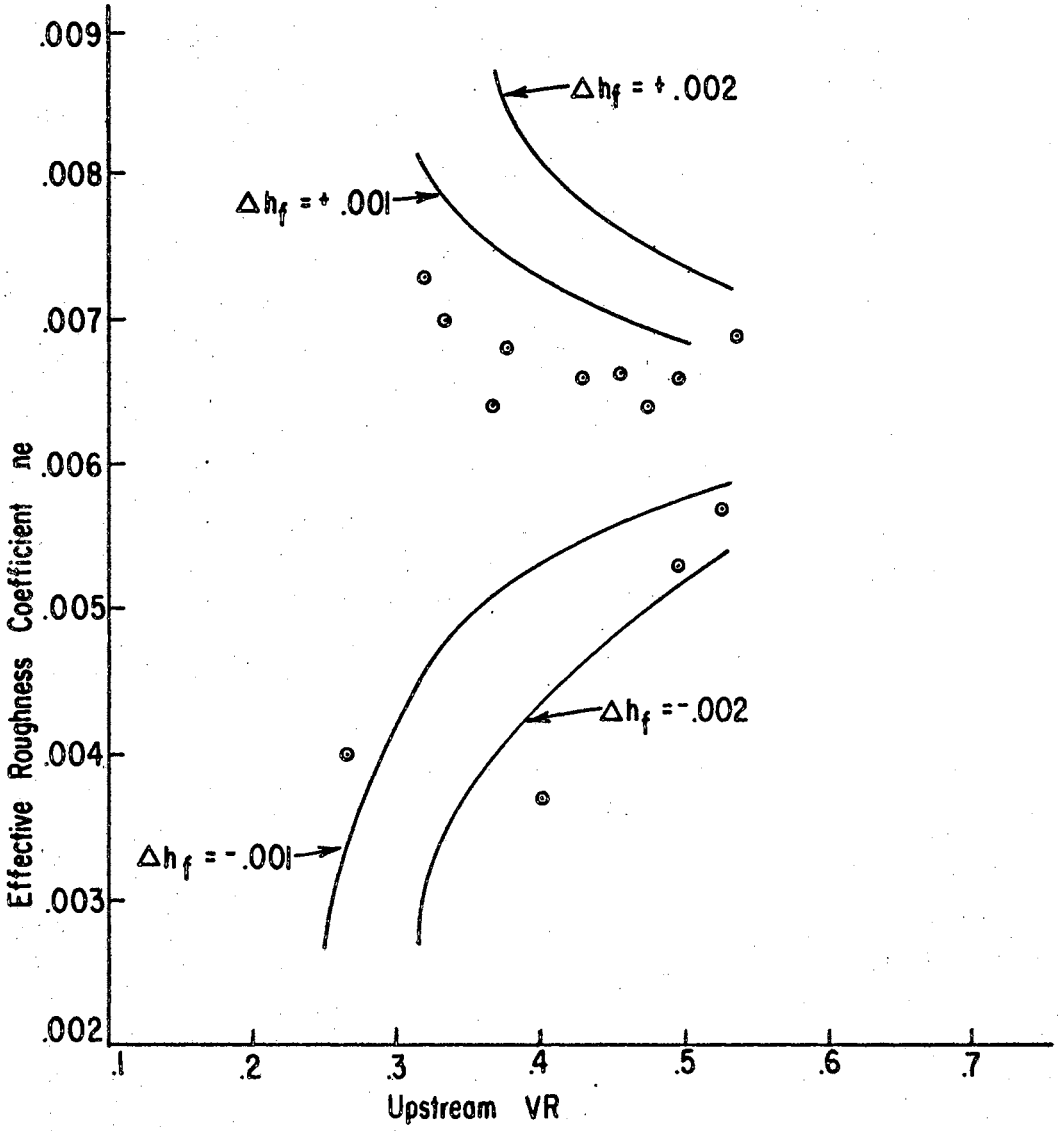

Figure 18. Tolerance Bands on the Mean of n_e (0.0073) for Water Surface Errors of $h_f = \pm 0.001, \pm 0.002$ ft., for Single Bay Tests

flows greater than 0.8530 measured outflow exceeded measured inflow.

(Note, outflow measurement for a bay was calculated as follows: The head, h, above the orifices at the six stations was measured by the common stilling well. Using these values of h and the calibration curve for weir and orifice flow, q's, at the respective stations were found. From the six values of q for each bay an average value of q was found for each bay. Total outflow from each bay was calculated by multiplying average q for a bay times the number of orifices in the bay. Total outflow from bay 1 plus total outflow from bay 2 gives total outflow from the channel.)

The following analysis indicated an error either in measuring entering flow or in H-Flume measurements. Since the inflow measuring device (orifice plate and manometer) is considered to be a much more sensitive measuring device (99.5 per cent accuracy) than the H-Flume (97 per cent accuracy) the error was thought to be with the H-Flume readings.

By readjusting the q values for a specific test by the per cent deviation between measured inflow and measured outflow, Figure 19 was arrived at. The results compare favorably with Barefoot's results and indicate that there was some error in H-Flume measurements. Figure 19 was used as the orifice and weir calibration curve.

For higher inflows in the two bay tests slightly lower orifice flows, q, were noted in the upstream bay as compared to orifice flows, q, at the same head in single bay tests. The downstream bay which was discharging the initial furrow flow behaved as in the single bay tests. This could possibly be caused by the higher velocities encountered in the first bay which is operating as the cut-back bay.

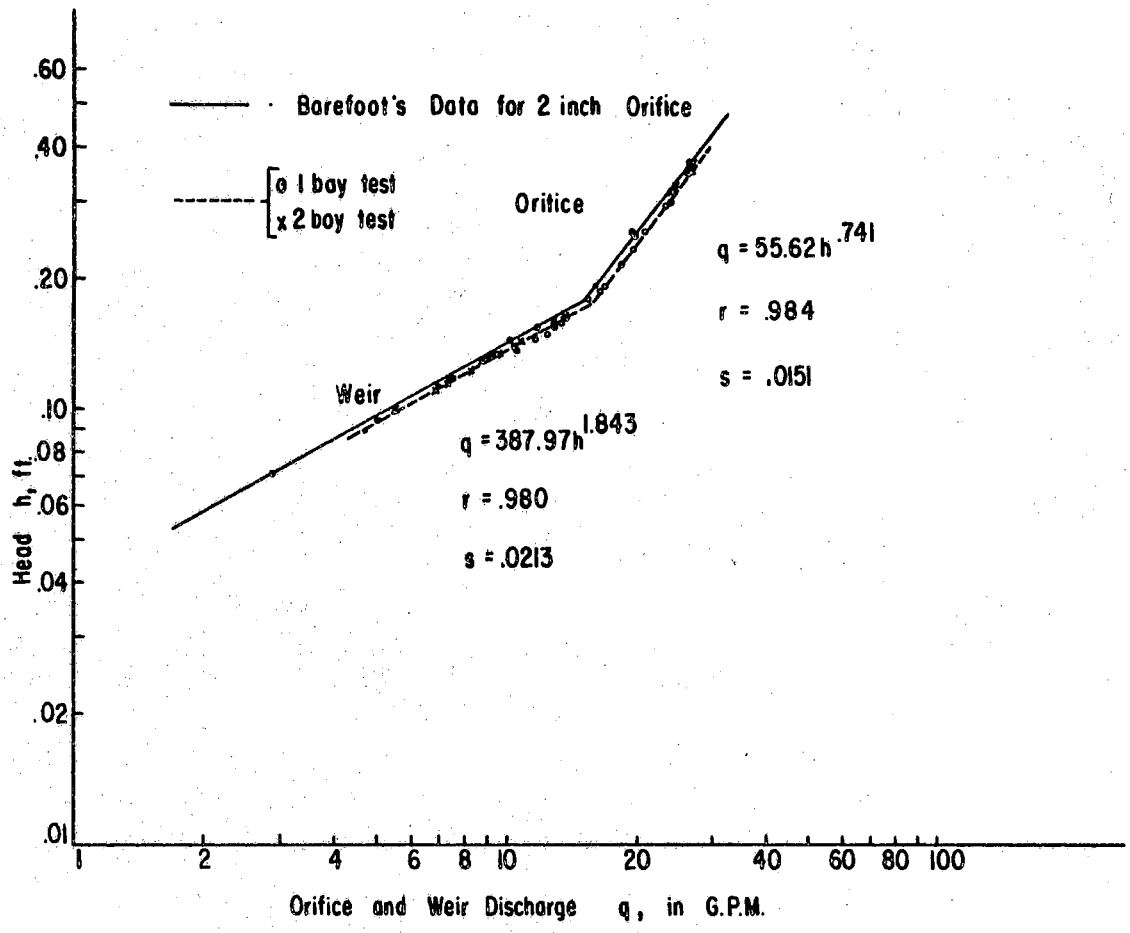

Figure 19. Head, h, Versus Weir and Orifice Flow q, Compared to Barefoot's Data

Figure 19 is a plot of head versus corrected flows for both weir and orifice flow. For weir flow the best fit equation is:

$$q = 387.97\ h^{1.843}$$

with a correlation coefficient r = .981 and standard deviation s = .02132.

For orifice flow the best fit equation is:

$$q = 55.626\ h^{.741}$$

with a correlation coefficient r = .984 and standard deviation s = .0152, where q is the orifice or weir flow in gallons per minute and h is the head of water in feet above the bottom of the orifice.

Water Surface Profiles for Spatially Varied Flow

Water surface profiles were measured for both single bay and two bay tests. Figure 20 is a plot of observed profiles and calculated profiles for single bay tests.

Water surface profiles were affected by two energy components which influence profile shape in a horizontal distribution channel, friction losses and velocity head recovery.

Rising profiles were observed in all the single bay tests. This is attributed to velocity head recovery exceeding friction loss which results from kinetic energy being converted to potential energy. As inflow Q increased from 0.538 c.f.s. to 1.579 c.f.s., the change in water surface elevation between the ends of the bay increased from 0.0015 ft. to 0.008 ft.

The calculated profiles were computed using Equation (2-17), an average value of computed $\bar{n}$ = 0.0126 was used for calculating profiles.

Water surface profiles for the two bay tests were measured and plotted in Figure 21. Two series of two bay tests were run. For one series both bays were 100 feet in length with a drop of 0.185 feet between bays. For the second set of tests, the downstream bay was 80 feet long with a drop of 0.219 feet between bays.

In all the two bay tests, falling profiles were observed in the upstream bay. This was caused by friction losses exceeding velocity head recovery.

Larger declines in the water surface profiles in the upstream bay were observed at lower inflow rates because friction losses predominated. This was because less per cent of the total outflow was discharged from the first bay for lower inflows and hence the rate of velocity change through the bay is slight. Whereas higher inflows resulted in more discharge from bay 1 and less of a falling profile.

For example the proportion of inflow remaining at the beginning of the downstream bay for the first series of tests decreased from 77 per cent to 61 per cent as flow increased from 1.95 c.f.s. to 2.60 c.f.s. For the inflow of 1.95 c.f.s., 23 per cent of the inflow was discharged in the upstream bay. The wide variation from 77 per cent to 61 per cent was because the downstream bay is discharging at the initial furrow flow and hence orifice flow is occurring, whereas the upstream bay is at cut-back flow and in most cases weir flow is occurring. Hence, a given increase in inflow will result in a greater percentage of that increase being discharged in the upstream bay.

Rising profiles were observed in the downstream bay and steeper profiles occurred as inflow increased as was the case in single bay tests.

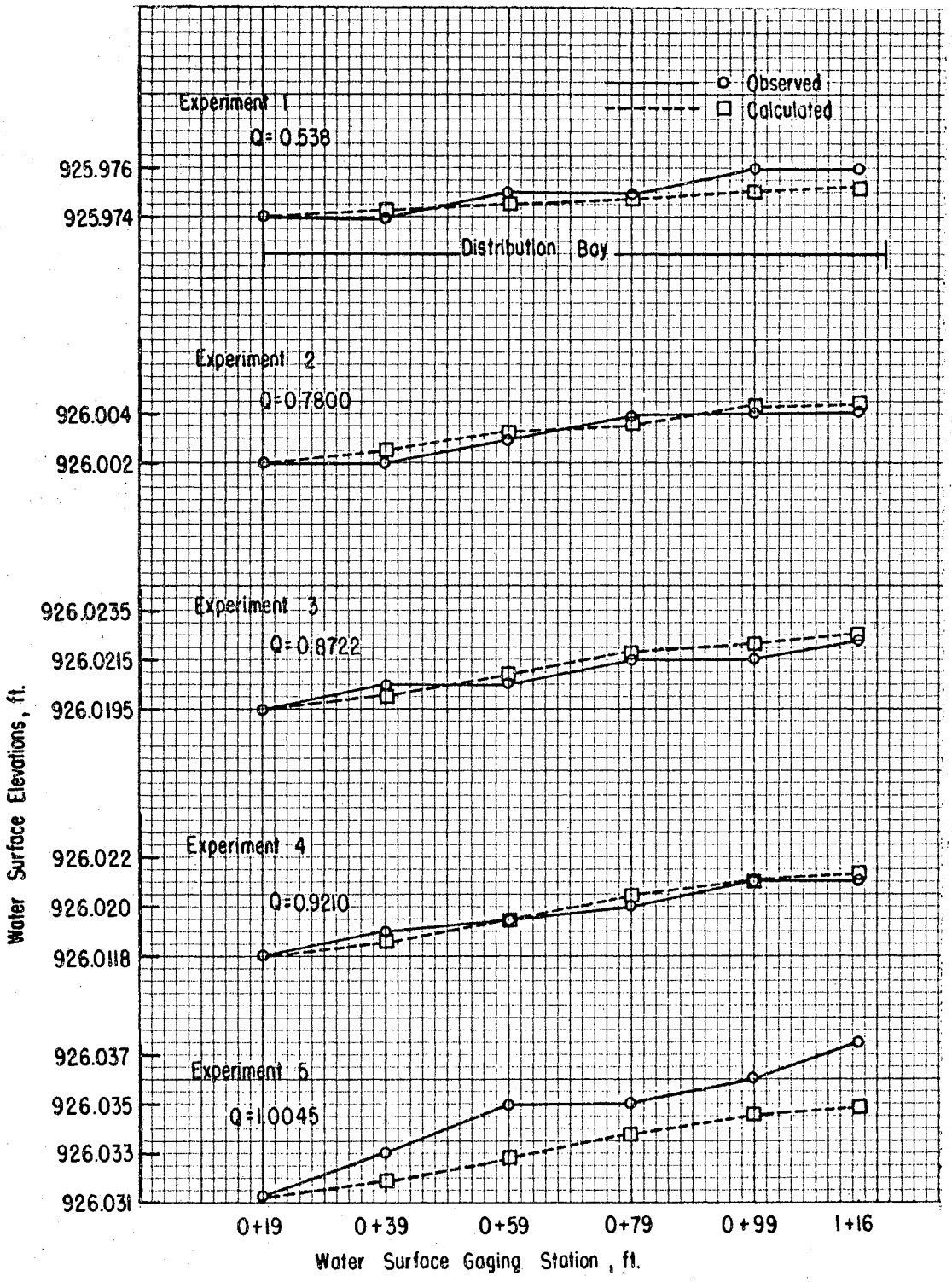

Figure 20. Observed and Calculated Water Surface Profiles for Decreasing Spatially Varied Flow in One Bay

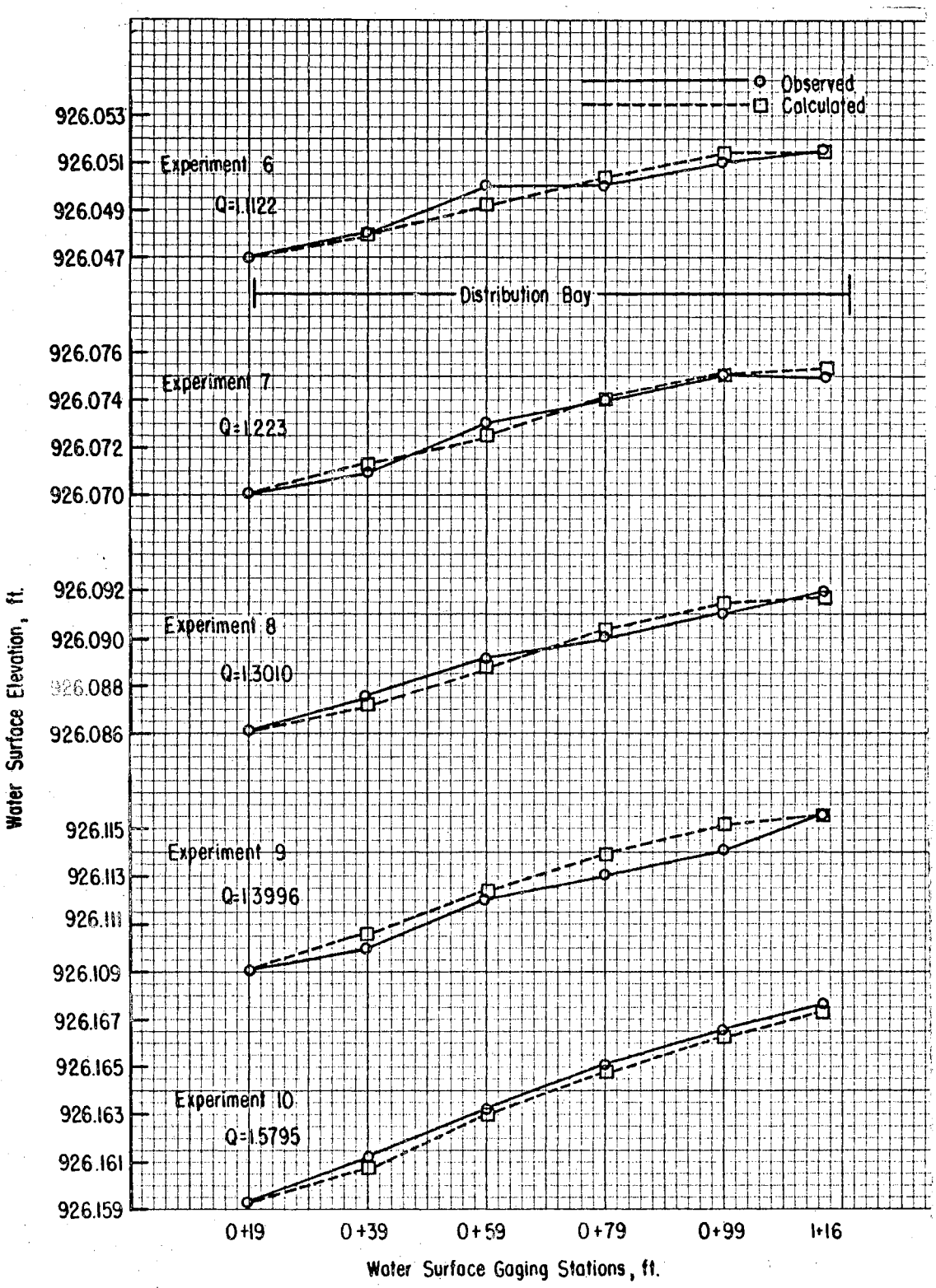

Figure 20. Observed and Calculated Water Surface Profiles for Decreasing Spatially Varied Flow in One Bay

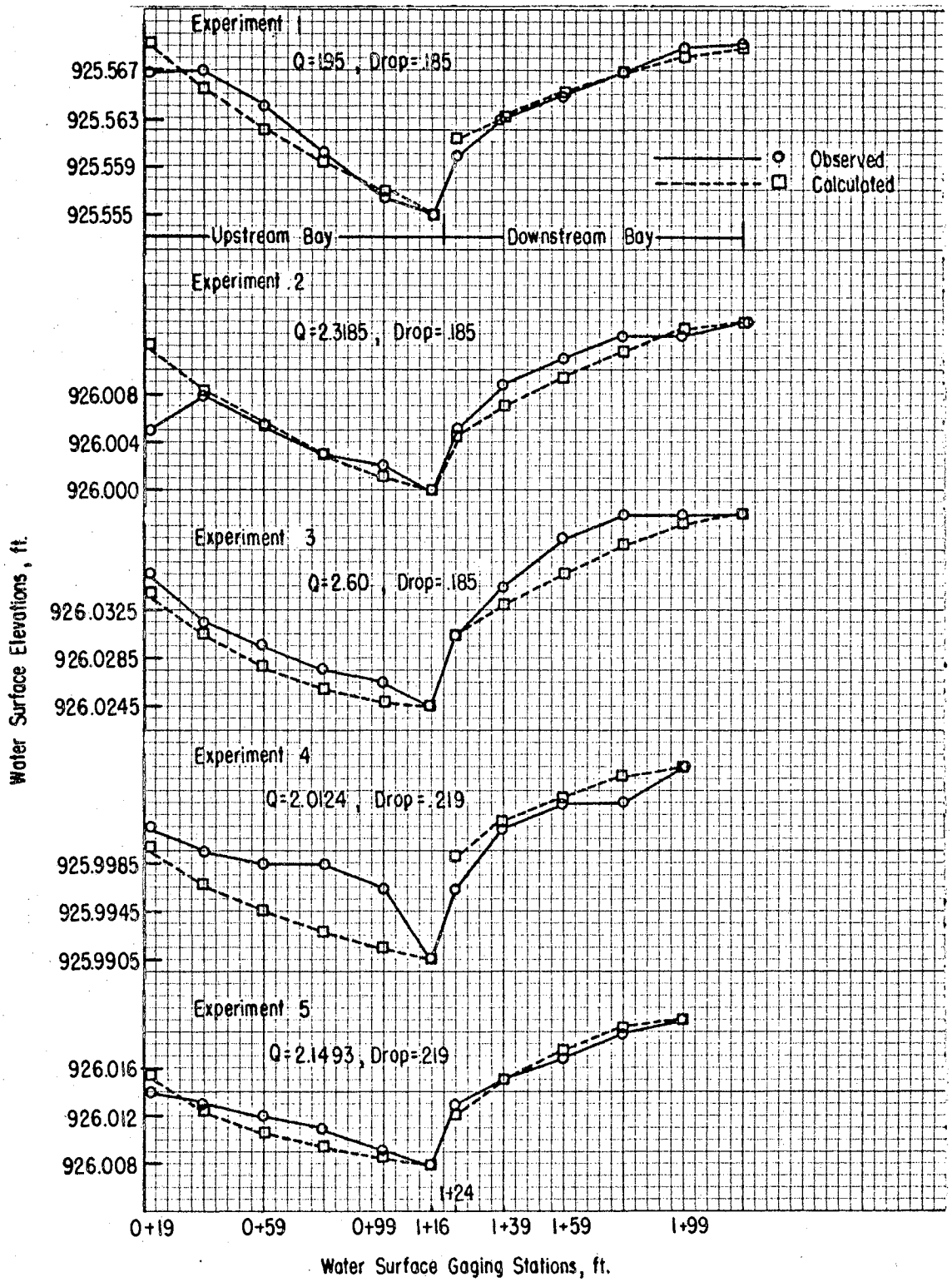

Figure 21. Observed and Calculated Water Surface Profiles for Decreasing Spatially Varied Flow in Two Bays

An overall rise in water surface elevation for the two bays occurred in all the tests.

The drop between the bays produced a change in velocity head Δhv which produced a rise in the water surface elevation somewhat less than Δhv. For example, in the experiment when inflow Q = 2.318 c.f.s., the expected change in velocity head Δhv = .0078 ft. and the observed change in velocity head Δhv = .005 ft., the .0028 ft. difference in elevation was lost due to turbulence and friction.

Water surface profiles were calculated for the two bay tests by using Equation (2-17) and using the method Sweeten (25) used in similar research. The main consideration was that an apparent or virtual length L_1' was used in solving for the upstream profiles, where L_1' was the length of bay necessary to completely discharge the inflow Q from the upstream bay.

Variations in Orifice and Weir Discharge

One problem with such a channel was that orifice elevations varied in a random fashion along the length of the channel. The variation was slight, for example, usually no greater than 0.01 feet. But orifice elevation variation when combined with rising or falling water surface profiles produced variations in weir and orifice discharge along a bay.

Weir and orifice discharge uniformity was determined for each experiment in the following manner: During an experiment, in either bay, head, h, for six orifices was measured. Using the calibration curve, Figure 19, and the six values of h, the values of orifice or weir flow were computed. This represented a random sample of flows

for one bay.

For a given bay, the per cent variation V_D was computed from the equation

$$V_D = \frac{q\ max - q\ min}{q\ max} \times 100$$

where q max is the maximum orifice or weir of flow in a bay and q min is the minimum flow in a bay. The values of V_D are listed in Table VI.

Larger variations were observed for weir flow as opposed to orifice flow and the largest variation occurred during the two bay tests in the upstream bay.

Generally as inflow increased, there was less variation in weir or orifice flow for both one bay and two bay tests.

TABLE VI

VARIATION IN WEIR AND ORIFICE DISCHARGE
WITH ONE AND TWO DISTRIBUTION BAYS

Q Entering Flow (cfs)	1st Bay (gpm) Discharge into Furrow		2nd Bay (gpm) Discharge into Furrow		Variation % of Max. Discharge 1st Bay	Variation % of Max. Discharge 2nd Bay
	Maximum	Minimum	Maximum	Minimum		
0.5381	8.196	6.837			16.50	
0.7267	11.353	9.668			14.80	
0.7800	11.980	11.225			6.30	
0.8536	13.300	11.580			12.90	
0.8722	13.617	12.300			9.67	
0.9213	14.290	13.177			7.79	
1.0045	15.740	14.220			9.60	
1.1122	16.850	16.400			2.37	
1.2234	18.540	18.070			2.53	
1.3009	19.750	19.190			2.83	
1.3996	21.540	20.660			4.10	
1.3996	21.470	20.579			4.19	
1.5219	23.180	22.690			2.10	
1.5795	24.198	23.300			3.70	
1.9500	6.994	5.359	23.180	22.134	23.30	4.50
2.0897	9.318	7.250	24.170	22.630	22.10	6.30
2.230	10.339	7.775	24.090	23.560	24.70	2.20
2.318	11.831	8.740	24.617	23.650	26.10	3.90
2.600	14.555	12.919	25.430	24.270	11.20	3.50
2.0174	10.403	7.763	26.490	25.973	25.30	1.90
2.1493	12.266	9.500	26.689	26.189	22.50	1.80
2.2668	13.696	11.350	26.647	26.319	16.70	1.20

CHAPTER VII

SUMMARY AND CONCLUSIONS

A sheet metal flume for automated cut-back irrigation was designed hydraulically and structurally and constructed using the best design of those tested.

The optimum hydraulic section was designed. A hydraulic design table and nomograph solution were computed. These design aids enable a planner to accurately select the best system for a given set of conditions.

Preceding the structural analysis, several types of designs were investigated considering the problems of ease of assemblage in the field, support of the channel in the field, and leakage. The basic design consists of a structural steel angle framework shown in Figure 7. Taking the basic framework selected, several combinations of material design were considered and investigated theoretically. From these investigations three structural steel angle frameworks were built and three sizes of sheet metal sections chosen. Six combinations were tested and the final design in Figure 7 was selected.

A 230 foot section was assembled in the field for testing. Values of Manning's n were determined from gradually varied flow tests for various flows and depths of flow. Decreasing spatially varied flow tests were run in one and two bays. Values of roughness coefficients $\bar{n}$ and n_e were determined, orifice and weir calibration

was determined, and discharge uniformity was calculated.

The average values of n, $\bar{n}$, and n_e computed for design purposes in initial flow bays or single bays were n = 0.0096, $\bar{n}$ = 0.0126, and n_e = 0.00730. The value of $\bar{n}$ for cut-back bays was $\bar{n}$ = 0.01065.

The equations for weir and orifice flow were determined; for weir flow, $q = 387.97\ h^{1.8435}$ and for orifice flow, $q = 55.62\ h^{0.7415}$, with h measured from the bottom of the orifice.

Uniformity of discharge was determined for the single and two bay tests. Variations from 2.1 per cent to 16.5 per cent occurred in the single bay tests. The median of the values was 8.29 per cent. For the two bay tests, the variation in the cut-back bay ranged from 11.2 per cent to 26.1 per cent with a median value of 21.5 per cent. Variation in the initial flow bay ranged from 1.2 per cent to 6.3 per cent with a median value of 3.16 per cent.

Water surface profiles were plotted from the observations made in the field. Water surface profiles were calculated for each test, using the average values of $\bar{n}$, and plotted for both single and two bay tests.

Conclusions

1. The hydraulic cross-section selected is a reasonable compromise.

2. Structurally the channel functions well. The supporting system is a functional design. The structural strength versus weight combinations seems to satisfy both the functions of strength and portability.

3. Orifice and weir calibration curves obtained compare favorably

with Barefoot's data for a 2.00 inch orifice.

4. Calculated and observed water surface profiles agree closely. Thus, $\bar{n} = 0.0126$ for the initial flow bay and $\bar{n} = 0.01065$ for the cut-back flow bay are satisfactory for design purposes. This also confirms the validity of Sweeten's (27) derivation of the equation for computing water surface profiles in two bays with a drop between them.

5. Measured values of velocity head conversion between bays were less than the theoretical values because of turbulence losses.

6. The ratio of $\bar{n}/n_{gvf} = 1.31$ for single bay tests compares with Sweeten's (24, 25) values of $\bar{n}/n_{gvf}$ for single bay tests run under similar conditions using siphon tubes and side weirs in a concrete trapezoidal irrigation channel. Sweeten obtained values of $\bar{n}/n_{gvf} = 1.28$ for siphon tube experiments, and $\bar{n}/n_{gvf} = 1.25$ for side weir experiments.

Suggestions for Future Research

1. A study of the effects of velocity rate past an orifice on discharge characteristics should be investigated.

2. A study of the operation of the system under an actual cropping situation would be desirable.

3. A more complete study of multi-bay tests is needed, where several lengths of bay are used, and the drop between bays is varied.

4. Values of $\bar{n}$ and n_e should be determined for single bays in which varying percentages of the entering flow are removed.

BIBLIOGRAPHY

1. American Institute of Steel Construction. Steel Construction Manual, New York, 1958.

2. American Iron and Steel Institute. Light Gage Cold-Formed Steel Design Manual, New York, 1962.

3. Barefoot, Armond D. "The Hydraulic Properties of Orifices and Circular Weirs with a 45 Degree Slope." Unpublished M. S. thesis, Agricultural Engineering Department, Oklahoma State University, 1968.

4. Bondurant, J. A. and A. S. Humphreys. "Surface Irrigation Through Automatic Control." Agricultural Engineering, Vol. 43 (January, 1962), pp. 20-21, 35.

5. Chow, Ven Te. Open Channel Hydraulics. New York: McGraw-Hill Book Company, Inc., 1959.

6. Collinge, Vincent K. "The Discharge Capacity of Side Weirs." Proceedings of the Institution of Civil Engineers, London, Vol. 6 (February, 1957), pp. 288-304.

7. Garton, J. E. "Automation of Cut-Back Furrow Irrigation." Unpublished Ph.D. dissertation, University of Missouri, Columbia, Missouri, 1964.

8. Garton, J. E. "Designing an Automatic Cut-Back Furrow Irrigation System." Oklahoma Agricultural Experiment Station, Bulletin B-651, October, 1966.

9. Garton, J. E., R. P. Beasley and A. D. Barefoot. "Automating of Cut-Back Furrow Irrigation." Agricultural Engineering, Vol. 45, No. 6 (June, 1964), pp. 328-29.

10. Greve, F. W. "Flow of Water Through Circular, Parabolic, and Triangular Vertical Notch-Weirs." Engineering Experiment Station Research, Series No. 40, Purdue University, Lafayette, Indiana, March, 1932.

11. Haise, H. R. and P. L. Whitney. "Hydraulically Controlled Gates for Automatic Surface Irrigation." Transactions of the American Society of Agricultural Engineers, Vol. 10, No. 5 (1967), pp. 639-44.

12. Henderson, F. M. Open Channel Flow. New York: The MacMillan Company, 1966.

13. Holtan, H. N., N. E. Minshall, and L. L. Harrold. Field Manual for Research in Agricultural Hydrology. Washington, D. C.: Agricultural Research Service, 1962.

14. Humphreys, A. S. "Control Structure for Automatic Surface Irrigation Systems." Transactions of the American Society of Agricultural Engineers, Vol. 10, No. 1 (1967), pp. 1-23, 27.

15. Israelson, Orson W. and V. E. Hansen. Irrigation Principles and Practice. 3rd edition. New York: John Wiley and Sons, Inc., 1962.

16. King, Horace W. Handbook of Hydraulics. 3rd edition. New York: McGraw-Hill Book Company, Inc., 1963.

17. Laurson, Philip G. and W. J. Cox. Mechanics of Materials. New York: John Wiley and Sons, Inc., 1948.

18. McCool, Don K. "Spatially Varied Steady Flow in a Vegetated Channel." Unpublished Ph.D. dissertation, Oklahoma State University, 1965.

19. Mink, A. L., J. E. Garton and J. M. Sweeten. "Hydraulics of an Irrigation Distribution Channel." Paper presented to the Southwest Section Meeting of the American Society of Agricultural Engineers, Stillwater, Oklahoma, April 26-28, 1967.

20. Mink, Albert L. "The Hydraulics of an Irrigation Distribution Channel." Unpublished Ph.D. dissertation, Agricultural Engineering Department, Oklahoma State University, 1967.

21. Parker, Harry. Simplified Engineering for Architects and Builders. New York: John Wiley and Sons, Inc., 1955.

22. Pope, David L. "Design of an Automatic Check Gate." Unpublished Report, Oklahoma State University, Fall, 1969.

23. Streeter, Victor L. Fluid Mechanics. New York: McGraw-Hill Book Company, Inc., 1962.

24. Sweeten, John M. "The Hydraulic Roughness of an Irrigation Channel with Decreasing Spatially Varied Flow." Unpublished M. S. thesis, Agricultural Engineering Department, Oklahoma State University, 1967.

25. Sweeten, J. M. "Hydraulics of a Side Weir Irrigation System." Unpublished Ph.D. dissertation, Agricultural Engineering Department, Oklahoma State University, 1969.

26. Sweeten, J. M., J. E. Garton, and A. L. Mink. "The Hydraulic Roughness of an Irrigation Channel with Decreasing Spatially Varied Flow." Paper presented at the National Winter Meeting of the American Society of Agricultural Engineers, Detroit, Michigan, December 12-15, 1967.

27. Sweeten, J. M. and J. E. Garton. "The Hydraulics of an Automated Furrow Irrigation System with Rectangular Side Weir Outlets." Paper presented at the National Summery Meeting of the American Society of Agricultural Engineers, W. Lafayette, Indiana, June 22-25, 1969.

28. Woodward, Sherman M. and C. J. Posey. Hydraulics of Steady Flow in Open Channels. New York: John Wiley and Sons, Inc., 1941.

APPENDIXES

APPENDIX A

HEAD AND DISCHARGE EXPERIMENTAL DATA

SINGLE BAY TESTS

	Orifice	Flow
	H	Q
(1)	0.1760	14.880
(2)	0.1800	15.148
(3)	0.1890	16.439
(4)	0.1920	16.640
(5)	0.2160	18.344
(6)	0.2190	18.540
(7)	0.2310	19.326
(8)	0.2340	19.520
(9)	0.2470	20.745
(10)	0.2530	21.140
(11)	0.2590	20.660
(12)	0.2610	20.793
(13)	0.2920	23.060
(14)	0.2940	23.180
(15)	0.3050	23.859

	Weir	Flow
	H	Q
(1)	0.1140	6.951
(2)	0.1180	7.410
(3)	0.1360	10.542
(4)	0.1400	11.280
(5)	0.1410	11.225
(6)	0.1440	11.670
(7)	0.1490	12.434
(8)	0.1525	12.980
(9)	0.1555	12.686
(10)	0.1590	13.335
(11)	0.1615	13.617
(12)	0.1630	13.960

TWO BAY TESTS

	Orifice	Flow
	H	Q
(16)	0.1710	13.825
(17)	0.1825	14.555
(18)	0.2860	22.430
(19)	0.2880	22.630
(20)	0.2980	23.180
(21)	0.3130	24.170
(22)	0.3210	23.684
(23)	0.3280	24.090
(24)	0.3320	23.936
(25)	0.3360	24.163
(26)	0.3595	26.260
(27)	0.3610	24.967
(28)	0.3635	26.490
(29)	0.3695	25.430
(30)	0.3750	26.357
(31)	0.3760	26.410
(32)	0.3815	26.420
(33)	0.3865	26.702

	Weir	Flow
	H	Q
(13)	0.1000	5.560
(14)	0.1120	6.870
(15)	0.1160	7.360
(16)	0.1230	8.220
(17)	0.1310	8.740
(18)	0.1325	9.200
(19)	0.1340	9.2684
(20)	0.1355	9.593
(21)	0.1370	9.500
(22)	0.1420	10.339
(23)	0.1460	10.070
(24)	0.1460	10.707
(25)	0.1610	12.710
(26)	0.1615	12.793
(27)	0.1665	13.540

APPENDIX B

EXPERIMENTAL DATA, ROUGHNESS COEFFICIENTS, OBSERVED AND CALCULATED FLOW PROFILES FOR DECREASING SPATIALLY VARIED FLOW TESTS

Experiment 1

$Q = 0.5381$ $\quad \bar{n} = 0.0087$ $\quad n_e = 0.0050$

Stations	Observed Water Surface Elevations	Calculated Water Surface Elevations
0 + 19	925.974	925.974
0 + 39	925.974	925.97424
0 + 59	925.975	925.97455
0 + 79	925.975	925.97485
0 + 99	925.976	925.9751
1 + 16	925.976	925.9752

Experiment 2

$Q = 0.7217$ $\quad \bar{n} = 0.0144$ $\quad n_e = 0.0083$

Stations	Observed Water Surface Elevations	Calculated Water Surface Elevations
0 + 19	926.002	925.002
0 + 39	926.0025	926.00243
0 + 59	926.003	926.00297
0 + 79	926.0035	926.0035
0 + 99	926.004	926.0039
1 + 16	926.004	926.0040

Experiment 3

$Q = 0.7800$ $\quad \bar{n} = 0.0139$ $\quad n_e = 0.0080$

Stations	Observed Water Surface Elevations	Calculated Water Surface Elevations
0 + 19	926.002	926.002
0 + 39	926.002	926.00249
0 + 59	926.003	926.0031
0 + 79	926.004	926.00375
1 + 16	926.004	926.00441

Experiment 4

$Q = 0.8722$ $\quad \bar{n} = 0.0129$ $\quad n_e = 0.0074$

Stations	Observed Water Surface Elevations	Calculated Water Surface Elevations
0 + 19	926.0195	926.0195
0 + 39	926.0205	926.02012
0 + 59	926.0205	926.02088
0 + 79	926.0215	926.0216
0 + 99	926.0215	926.0222
1 + 16	926.0225	926.02242

Experiment 5

$Q = 0.9213$ $\quad \bar{n} = 0.0135$ $\quad n_e = 0.0078$

Stations	Observed Water Surface Elevations	Calculated Water Surface Elevations
0 + 19	926.018	926.018
0 + 39	926.019	926.01869
0 + 59	926.0195	926.01954
0 + 79	926.020	926.0203
0 + 99	926.021	926.02101
1 + 16	926.021	926.02126

Experiment 6

$Q = 1.0045$ $\quad \bar{n} = 0.0082$ $\quad n_e = 0.0047$

Stations	Observed Water Surface Elevations	Calculated Water Surface Elevations
0 + 19	926.031	926.031
0 + 39	926.033	926.03182
0 + 59	926.035	926.0328
0 + 79	926.035	926.03379
0 + 99	926.036	926.03452
1 + 16	926.0375	926.03481

Experiment 7

$Q = 1.1122$ $\quad \bar{n} = 0.0131$ $\quad n_e = 0.0076$

Stations	Observed Water Surface Elevations	Calculated Water Surface Elevations
0 + 19	926.047	926.047
0 + 39	926.048	926.04799
0 + 59	926.050	926.04921
0 + 79	926.050	926.05034
0 + 99	926.051	926.05121
1 + 16	926.0515	926.05156

Experiment 8

$Q = 1.2234$ $\quad \bar{n} = 0.0132$ $\quad n_e = 0.00766$

Stations	Observed Water Surface Elevations	Calculated Water Surface Elevations
0 + 19	926.070	926.070
0 + 39	926.071	926.07118
0 + 59	926.073	926.07258
0 + 79	926.074	926.07393
0 + 99	926.075	926.07494
1 + 16	926.075	926.07534

Experiment 9

$Q = 1.3009$ $\quad \bar{n} = 0.0129$ $\quad n_e = 0.0074$

Stations	Observed Water Surface Elevations	Calculated Water Surface Elevations
0 + 19	926.086	926.086
0 + 39	926.0875	926.08732
0 + 59	926.0885	926.08886
0 + 79	926.0900	926.09033
0 + 99	926.0910	926.09143
1 + 16	926.0920	926.09186

Experiment 10

$Q = 1.3996$ $\quad \bar{n} = 0.0131$ $\quad n_e = 0.0076$

Stations	Observed Water Surface Elevations	Calculated Water Surface Elevations
0 + 19	926.109	926.109
0 + 39	926.110	926.11051
0 + 59	926.112	926.11226
0 + 79	926.112	926.11392
0 + 99	926.114	926.11516
1 + 16	926.1155	926.11564

Experiment 11

$Q = 1.3996$ $\quad \bar{n} = 0.0109$ $\quad n_e = 0.0063$

Stations	Observed Water Surface Elevations	Calculated Water Surface Elevations
0 + 19	926.1115	926.1115
0 + 39	926.114	926.11299
0 + 59	926.116	926.11471
0 + 79	926.118	926.11634
0 + 99	926.120	926.11755
1 + 16	926.120	926.11802

Experiment 12

$Q = 1.5219$ $\quad \bar{n} = 0.0116$ $\quad n_e = 0.0667$

Stations	Observed Water Surface Elevations	Calculated Water Surface Elevations
0 + 19	926.144	926.144
0 + 39	926.147	926.14573
0 + 59	926.150	926.14770
0 + 79	926.152	926.14954
0 + 99	926.152	926.15091
1 + 16	926.153	926.15144

Experiment 13

$Q = 1.5795$ $\quad \bar{n} = 0.0129$ $\quad n_e = 0.0079$

Stations	Observed Water Surface Elevations	Calculated Water Surface Elevations
0 + 19	926.159	926.159
0 + 39	926.161	926.16085
0 + 59	926.163	926.16293
0 + 79	926.164	926.16488
0 + 99	926.1665	926.16633
1 + 16	926.167	926.16689

Experiment 1

Q = 1.95	$\bar{n}$ for First Bay = 0.009989	Length of Second Bay = 100 ft.
Stations	Observed Water Surface Elevations	Calculated Water Surface Elevations
0 + 19	925.967	925.96919
0 + 39	925.967	925.96539
0 + 59	925.964	925.96210
0 + 79	925.960	925.95929
0 + 99	925.9565	925.95694
1 + 16	925.955	925.955
1 + 24	925.960	925.96148
1 + 41	925.963	925.96337
1 + 61	925.965	925.96538
1 + 81	925.967	925.96729
2 + 01	925.969	925.9685
2 + 21	925.969	925.969

Experiment 2

Q = 2.0897	$\bar{n}$ for First Bay = 0.01021	Length of Second Bay = 100 ft.
Stations	Observed Water Surface Elevations	Calculated Water Surface Elevations
0 + 19	925.9835	925.9823
0 + 39	925.983	925.9791
0 + 59	925.980	925.9765
0 + 79	925.978	925.9745
0 + 99	925.976	925.973
1 + 16	925.972	925.972
1 + 24	925.977	925.97970
1 + 41	925.981	925.98161
1 + 61	925.985	925.98353
1 + 81	925.985	925.98527
2 + 01	925.985	925.98652
2 + 21	925.987	925.987

Experiment 3

Q = 2.23	$\bar{n}$ for First Bay = 0.01016	Length of Second Bay = 100 ft.
Stations	Observed Water Surface Elevations	Calculated Water Surface Elevations
0 + 19	925.998	926.0012
0 + 39	925.998	925.9975
0 + 59	925.997	925.9945
0 + 79	925.994	925.9921
0 + 99	925.991	925.9903
1 + 16	925.989	925.989
1 + 24	925.9965	925.99555
1 + 41	925.999	925.9977
1 + 61	926.001	925.99996
1 + 81	926.003	926.00198
2 + 01	926.003	926.00344
2 + 21	926.004	926.004

Experiment 4

Q = 2.318	$\bar{n}$ for First Bay = 0.01045	Length of Second Bay = 100 ft.
Stations	Observed Water Surface Elevations	Calculated Water Surface Elevations
0 + 19	926.005	926.0124
0 + 39	926.008	926.0084
0 + 59	926.005	926.0044
0 + 79	926.003	926.003
0 + 99	926.002	926.0013
1 + 16	926.000	926.000
1 + 24	926.005	926.0051
1 + 41	926.009	926.00736
1 + 61	926.011	926.00974
1 + 81	926.013	926.01188
2 + 01	926.013	926.01341
2 + 21	926.014	926.0140

Experiment 5

Q = 2.60	$\bar{n}$ for First Bay = 0.01083	Length of Second Bay = 100 ft.
Stations	Observed Water Surface Elevations	Calculated Water Surface Elevations
0 + 19	926.0355	926.03319
0 + 39	926.0315	926.03063
0 + 59	926.0295	926.02802
0 + 79	926.0275	926.02620
0 + 99	926.0265	926.02504
1 + 16	926.0245	926.0245
1 + 24	926.0305	926.03070
1 + 41	926.0345	926.03222
1 + 61	926.0385	926.03584
1 + 81	926.0405	926.03818
2 + 01	926.0405	926.03986
2 + 21	926.0405	926.0405

Experiment 6

Q = 2.0124	$\bar{n}$ for First Bay = 0.01094	Length of Second Bay = 80 ft.
Stations	Observed Water Surface Elevations	Calculated Water Surface Elevations
0 + 19	926.0015	925.99961
0 + 39	925.9995	925.99677
0 + 59	925.9985	925.99448
0 + 79	925.9985	925.99271
0 + 99	925.9965	925.99140
1 + 16	925.9905	925.99050
1 + 24	925.9965	925.99913
1 + 41	926.0015	926.00178
1 + 61	926.0035	926.00415
1 + 81	926.0035	926.00585
2 + 01	926.0065	926.00650

Experiment 7

Q = 2.1493 $\bar{n}$ for First Bay = 0.01070 Length of Second Bay = 80 ft.

Stations	Observed Water Surface Elevations	Calculated Water Surface Elevations
0 + 19	926.014	926.01548
0 + 39	926.013	926.01284
0 + 59	926.012	926.01084
0 + 79	926.011	926.00948
0 + 99	926.009	926.00848
1 + 16	926.008	926.00800
1 + 24	926.013	926.01252
1 + 41	926.015	926.01522
1 + 61	926.017	926.01762
1 + 81	926.019	926.01934
2 + 01	926.020	926.02000

Experiment 8

Q = 2.2668 $\bar{n}$ for First Bay = 0.01081 Length of Second Bay = 80 ft.

Stations	Observed Water Surface Elevations	Calculated Water Surface Elevations
0 + 19	926.0185	926.01996
0 + 39	926.0195	926.01766
0 + 59	926.0205	926.01604
0 + 79	926.0165	926.01503
0 + 99	926.0155	926.01452
1 + 16	926.0145	926.01450
1 + 24	926.0205	926.01845
1 + 41	926.0245	926.02135
1 + 61	926.0255	926.02394
1 + 81	926.0255	926.02579
2 + 01	926.0265	926.0265

NOMENCLATURE

A	Cross sectional area of channel, ft^2
A_{avg}	Average area, ft^2
B	Momentum coefficient
C	Constant
d	Depth normal to channel bottom, ft.
D	Orifice diameter, ft.
D	Hydraulic depth, ft.
Fr	Froude number
F_f	Total external force of friction, lbs.
g	Acceleration of gravity, ft/sec^2
h_1	Head for initial furrow flow, ft.
h_2	Head for cut-back furrow flot, ft.
h	Head above bottom of orifice, ft.
h_f	Loss of energy head, ft.
h_f'	Measure of external head losses due to friction, ft.
H	Total energy head, ft.
H	Head above orifice invert, ft.
Δh_v	Velocity head recovery, ft.
i	Subscript referring to upstream end of irrigation bay
K	Empirical constant
L	Empirical constant
L	Length of irrigation bay, ft.
L_1'	Virtual channel length, ft.

L_s Orifice or weir spacing, ft.

M Empirical exponent

N Empirical exponent

N_{RE} Reynold's number

n Manning's roughness coefficient, $ft^{1/6}$

$\bar{n}$ Mean roughness coefficient, $ft^{1/6}$

n_e Effective roughness coefficient, $ft^{1/6}$

o Subscript referring to downstream end of irrigation bay

P Pressure, lb/ft^2

q Discharge per foot of length, $ft^3/sec/ft$.

q Weir and orifice discharge, ft^3/sec.

q_1 Initial furrow flow, ft^3/sec.

q_2 Cut-back furrow flow, ft^3/sec.

Q Channel inflow, ft^3/sec.

Q_{W1} Flow from one siphon tube or weir, ft^3/sec.

R Hydraulic radius, ft.

r Correlation coefficient

R_{avg} Average hydraulic radius, ft.

s Standard deviation

S_{fe} Effective energy slope

S_o Channel bottom slope

S Slope of energy line

S Field slope

t Time, sec.

T Top width, ft.

V Channel velocity, ft/sec.

V_D Variation in orifice and weir discharge, per cent

w Unit weight of water, lbs/ ft^3

W Compensation for wave action in channel, ft.

WS_i Water surface elevation at upstream end of irrigation bay, ft.

WS_o Water surface elevation at downstream end of irrigation bay, ft.

ΔWS Difference in water surface elevation between an upstream station and a downstream station, ft

X Coordinate in direction of flow, ft

ΔX Distance between siphon tubes, weir plates, or orifices in an irrigation distribution channel, ft

Y Depth of flow, ft

z Vertical distance from datum, ft

z Drop between bays, ft

α Coriolis coefficient

θ Inclination angle of channel bottom

VITA

Vincent William Uhl, Jr.

Candidate for the Degree of

Master of Science

Thesis: A SEMI-PORTABLE SHEET METAL FLUME FOR AUTOMATED IRRIGATION

Major Field: Agricultural Engineering

Biographical:

Personal Data: Born at Darby, Pennsylvania, January 23, 1945, the son of Vincent W. and Francis K. Uhl.

Education: Graduated from St. Joseph's Prep School in Philadelphia, Pennsylvania, in 1962; attended the University of Notre Dame in 1962, and graduated with a Bachelor of Science degree in Mechanical Engineering from Notre Dame in 1966. Completed the requirements for the Master of Science degree in May, 1970.

Professional Experience: Worked as a Peace Corps Volunteer in Gujarat, India, in the area of Agricultural Education and Extension from August, 1966, to August, 1968; Graduate Teaching Assistant from September, 1968, to January, 1969, and Graduate Research Assistant from February, 1969, to January, 1970.

Professional and Honorary Organizations: Member of Mechanical Engineering Honorary Fraternity, Pi Tau Sigma.